PCT

(51) International Patent Classification ^{6} :		(11) International Publication Number:	**WO 99/36779**
G01N 33/533	**A1**	(43) International Publication Date:	22 July 1999 (22.07.99)

(21) International Application Number: PCT/US99/00774

(22) International Filing Date: 14 January 1999 (14.01.99)

(30) Priority Data:
09/007,167 14 January 1998 (14.01.98) US

(71)(72) Applicant and Inventor: LAKOWICZ, Joseph, R. [US/US]; 10037 Fox Den Road, Ellicott City, MD 21042 (US).

(72) Inventors: CASTELLANO, Felix; Apartment 401, 7660 Woodpark Lane, Columbia, MD 21046 (US). MURTAZA, Zakir; 900 South Paca Street, Baltimore, MD 21230 (US).

(74) Agents: REPPER, George, R. et al.; Rothwell, Figg, Ernst & Kurz, Suite 701 East, Columbia Square, 555 13th Street N.W., Washington, DC 20004 (US).

(81) Designated States: CA, JP, European patent (AT, BE, CH, CY, DE, DK, ES, FI, FR, GB, GR, IE, IT, LU, MC, NL, PT, SE).

Published
With international search report.
Before the expiration of the time limit for amending the claims and to be republished in the event of the receipt of amendments.

(54) Title: METHOD OF CONDUCTING AN ASSAY OF A SAMPLE CONTAINING AN ANALYTE OF INTEREST

(57) Abstract

In accordance with the present invention, a method of conducting an assay of a sample containing an analyte of interest includes the step of forming a mixture so as to bring a metal–ligand complex into interactive proximity with the sample containing the analyte of interest. The mixture is irradiated with electromagnetic light energy so as to cause emission of light indicative of the analyte of interest. The emitted light is measured, and the measurement of the emitted light is utilized to measure the analyte of interest. The metal–ligand complex can be $[Re(bcp)(CO)_3(4\text{--}COOHPy)]^+$, $[Os(phen)_2(aphen)]^{2+}$, $[Os(tpy)(triphos)]^{2+}$, $[Os(tppz)_2]^{2+}$, and $[Os(ttpy)_2]^{2+}$, or the like. Also, the present invention is directed to a metal–ligand complex of the formula $[Re(bcp)(CO)_3(4\text{--}COOHPy)]^+$.

METHOD OF CONDUCTING AN ASSAY OF A
SAMPLE CONTAINING AN ANALYTE OF INTEREST

BACKGROUND OF THE INVENTION

Field of the Invention

5   The present invention is in the field of
conducting an assay of a sample containing an analyte
of interest.

Description of the Background Art

       In recent years there has been increased interest
10   in the synthesis, characterization and application of
metal-ligand complexes in biomolecule research. In
addition to their use as photosensitizers, metal-ligand
complexes have been used as luminescence probes in
polymers. For instance, metal-containing intercalators
15   such as square-planar platinum(II) complexes containing
aromatic terpyridine or phenanthroline ligands have
been used in probing DNA structure and the
intercalation process itself. The reagent
methidiumpropyl-Fe(II) EDTA, which contains a redox-
20   active metal center tethered to an organic
intercalator, has been applied in "footprinting"
experiments to determine the sequence specificity of
small drugs bound to DNA. Ru(II) and Os(II) transition
metal compounds have been used to probe DNA structure
25   and study long-range electron transfer.
       More recent studies have shown that ruthenium
(Ru(II)), rhenium (Re(I)) and osmium (Os(II)) metal-
ligand complexes display high anisotropy in the absence
of rotational diffusion. Importantly, metal ligand

complexes display luminescence decay times ranging from 100 ns to 100 µs. Consequently, these probes extend the observable timescale of anisotropy decay measurements by orders of magnitude compared with that

5   observable with routinely used organic fluorophores. As a result of this, metal-ligand complexes have been used to probe the microsecond dynamics of DNA. In addition, time-resolved anisotropy measurements of proteins can be extended to the microsecond timescale

10   using metal-ligand complexes. Intensity and anisotropy decays of Ru(II) metal-ligand complexes when covalently linked to human serum albumin, concanavalin A, human immunoglobulin G and ferritin demonstrated that this class of probes could be used to measure rotational

15   motions from 10 ns to 1.5 µs, which so far has been inaccessible using the classical organic fluorophores. Fluorescence polarization immunoassays using metal-ligand complexes covalently bound to human serum albumin (as the antigen) demonstrated the potential use

20   of metal-ligand complexes in fluorescence polarization immunoassays of high-molecular-weight analytes.

Fluorescence polarization (FP) was first theoretically described by Perrin in 1926, which was subsequently expanded and measured by Weber. Dandliker

25   and co-workers adapted FP for use in analytical biochemistry including antigen (Ag) - antibody (Ab) interactions, and hormone-receptor interactions. Since establishment of the theory and method by Dandliker, the use of FPI's (fluorescence polarization

30   immunoassays) for the quantitative and qualitative measurement of various types of molecules and bioconjugates has been reported. These include therapeutic drug monitoring, determination of hormones, drugs of abuse, proteins and peptides, proteases and

2

inhibitors, as well as DNA binding interactions. In fact, FPI technology is presently in widespread commercial use in several instruments.

5   A serious limitation of present immunoassays is that they are limited to low molecular weight antigens. This limitation is a result of the use of fluorophores, such as fluorescein, which display lifetimes near 4 ns. A FPI requires that emission from the unbound labeled antigen be depolarized, so that an increase in

10   polarization may be observed upon antigen binding to antibody. For depolarization to occur, the antigen must display a rotational correlation time much shorter than the lifetime of the probe (in the case of fluorescein, less than 4 ns) which limits the dynamic

15   range of the FPI to antigens with low molecular weights (Figure 16). Some long lifetime fluorophores, such as chelates of Eu^{3+} and Tb^{3+} have been used in time-resolved immunoassays, but they do not display polarized emission and are thus not useful in FPI's.

20   More recent studies have shown that $[Ru(bpy)_2(dcb)]^{2+}$, where bpy is 2,2'-bipyridine and dcb is 4,4'-dicarboxylic acid-2,2'-bipyridine, displays high polarization in the absence of rotational diffusion (~ 0.25), as well as a long lifetime (~ 400

25   ns). The experimental results demonstrated that the steady-state polarization of $[Ru(bpy)_2(dcb)]^{2+}$ labeled to HSA was sensitive to the binding of anti-HSA, which resulted in a 200% increase in polarization. Another metal-ligand complex, $[Os(bpy)_2(dcb)]^{2+}$, was also used

30   in a FPI to detect a high molecular weight bioconjugate using red excitation and emission wavelengths.

Many different approaches have been used to circumvent the present limitation of FPI's to low molecular weight substances. An early attempt to

3

develop FPI's for high molecular weight antigens was reported by Grossman. The dansyl (dimethylaminonaphthalene sulfonic acid) fluorophore was used because of its lifetime near 20 ns. Tsuruoka

5   and coworkers attempted to develop a FPI with IgG by increasing the molecular weight of the antibody. This was accomplished by immobilizing the antibody with latex or colloidal silver. Urios and Cittanova decreased the size of the labeled antibody by using Fab

10   fragments in place of complete IgG molecules. Another approach to enable the measurement of high-molecular-weight antigens was introduced by Wei and Herron. They used a tetramethylrhodamine-labeled synthetic peptide, which has a high binding affinity for the Ab of hCG

15   (human chorionic gonadotrophin), as the tracer antigen in their FPI for hCG. In the assay, the tracer antigen, which has a low molecular weight, is replaced by hCG (high molecular weight) thus reducing the amount of polarization.

20   Since the basic theory of the depolarization of fluorescence through Brownian rotation was presented by Perrin in 1926, fluorescence anisotropy decay measurements have been widely used to study the rotational dynamics of proteins, membrane-bound

25   proteins and other macromolecules. The use of the polarization of extrinsic fluorescent labels to study proteins was introduced by Weber and was applied to the characterization of a number of proteins by Weber and others.

30   There are limitations imposed by the short fluorescence lifetime that have been circumvented by use of phosphorescence anisotropy decays, which have been used to study the rotational dynamics of membrane-bound proteins. Such measurements are based

4

SUBSTITUTE SHEET (RULE 26)

exclusively on the triplet probe eosin, which displays a millisecond phosphorescence decay time in the absence of oxygen. Rotational motions have been quantified by transient absorption anisotropy and by time-resolved

5 phosphorescence anisotropy. There are, however, relatively few useful triplet probes. The use of phosphorescence is also inconvenient because of the need to rigorously exclude molecular oxygen, and the low initial phosphorescence anisotropies, typically 0.1

10 or smaller.

The polarized luminescence from metal ligand complexes has been used to study macromolecular dynamics. Studies have shown that ruthenium (Ru), rhenium (Re) and osmium (Os) metal ligand complexes

15 display high anisotropy in the absence of rotational diffusion. Importantly, these metal ligand complexes display luminescence decay times ranging from 100 ns to 100 μs. Consequently, these probes extend the observable timescale of anisotropy decay measurements

20 by many-fold compared with that observable with routinely used fluorophores. As a result, metal ligand complexes have been used to measure rotational motion of proteins and probe the submicrosecond dynamics of DNA. Time-resolved anisotropy measurements have

25 demonstrated that metal ligand complexes when covalently linked to human serum albumin (HSA), concanavalin A, human immunoglobin G, and ferritin can be used to measure rotational motions on the 10 ns to 1.5 μs timescale.

30 Conventional organic fluorophores typically have a lifetime in the range of 1-10 ns, generally absorb in the high energy range, and are not very photostable. These properties limit the ability of these fluorophores to study slower domain-to-domain motions

5

in proteins or the rotational motions of membrane-bound
proteins. Furthermore the sensitivity of these
fluorophores is also limited by interfering
autofluorescence which also occurs at the 1-10 ns time

5   scale.

          There remains a need in the art for metal-ligand
complex probes which display long absorption emission
wavelengths, long lifetimes, high luminescence, and/or
high quantum yields, for use as biomolecular probes,

10   and/or for metal-ligand complex probes that can be used
in fluorescence polarization immunoassays of high
molecular weight analytes, and for metal-ligand complex
probes that can be used as anisotropy probes for
protein hydrodynamics.

15   SUMMARY OF THE INVENTION

          In accordance with the present invention, a method
of conducting an assay of a sample containing an
analyte of interest includes the step of forming a
mixture so as to bring a metal-ligand complex into

20   interactive proximity (10 to 120 A°) with the sample
containing the analyte of interest. The mixture is
irradiated with electromagnetic light so as to induce
emission of light indicative of the analyte of
interest. The emitted light is measured, and the

25   measurement of the emitted light is utilized to measure
the analyte of interest. In accordance with one
embodiment, the metal-ligand complex is selected from
the group consisting of $[Re(bcp)(CO)_3(4-COOHPy)]^+$,
$[Os(phen)_2(aphen)]^{2+}$, $[Os(tpy)(triphos)]^{2+}$, $[Os(tppz)_2]^{2+}$,

30   and $[Os(ttpy)_2]^{2+}$.

6

BRIEF DESCRIPTION OF THE DRAWINGS

FIG. 1 shows the molecular structure of [Re(bcp)(CO)₃(4-COOHPy)]', which displays a high quantum yield near 0.5 in organic solutions and a lifetime near

5   7μs.

FIG. 2 is a graph depicting the absorption and emission spectra of [Re(bcp)(CO)₃(4-COOHPy)]' in CHCl₃, CH₃CN, CH₃OH, and in buffer, at room temperature. The excitation wavelength was 400 nm. The solid line shows

10   the excitation anisotropy spectrum in 100% glycerol at -60°C, with the emission wavelength tuned to 550 nm. The bandpass was 8 nm for all measurements.

FIG.3 graphically shows that in organic solutions, [Re(bcp)(CO)₃(4-COOHPy)]' is highly sensitive to

15   dissolved oxygen, but in the absence of dissolved oxygen, it displays a lifetime over 7 μs. The oxygen dependent spectra of the rhenium complex was taken at room temperature, excitation was 400 nm, and with a bandpass of 8 nm. The inset shows spectra obtained in

20   air and oxygen.

FIG. 4 graphically shows the frequency-domain intensity decays of [Re(bcp)(CO)₃(4-COOHPy)]' in methanol. The lifetime is reduced to about 0.5 microseconds in the presence of dissolved oxygen from

25   the atmosphere. The excitation was 390 nm and a 500 nm cutoff filter was used to isolate the emission.

FIG. 5 graphically shows the emission spectra of [Re(bcp)(CO)₃(4-COOHPy)]⁺ when conjugated to phosphatidyl ethanolamine and embedded into DPPG

30   vesicles. The mole ratio of the rhenium complex to phosphatidyl ethanolamine was 1:80. The excitation was 400 nm with a bandpass of 8 nm, measured at 20°C.

7

FIG. 6 graphically shows the lifetimes of [Re(bcp)(CO)$_3$(4-COOHPy)]$^+$ labeled DPPG vesicles measured by the frequency-domain or phase-modulation method. Excitation was 340 nm and a 470 nm cutoff filter was used to isolate the emission.

FIG. 7 graphically shows that similar favorable properties were found for [Re(bcp)(CO)$_3$(4-COOHPy)]$^+$ when conjugated to human serum albumin (HSA). The rhenium complex was conjugated to HSA in 0.1 M PBS buffer, pH 7.0, and equilibrated with argon or air. The excitation wavelength was 400 nm with a bandpass of 8 nm, at 20° C.

FIG. 8 graphically shows that the lifetime of [Re(bcp)(CO)$_3$(4-COOHPy)]$^+$ when conjugated to HSA is near 3 μs in the presence or absence of dissolved oxygen from the atmosphere. The excitation was 390 nm and a 500 nm cutoff filter was used to isolate the emission.

FIG. 9 graphically depicts binding of [Re(bcp)(CO)$_3$(4-COOHPy)]$^+$ labeled HSA to anti-HSA. The increase in polarization is due to binding of the antibody to HSA. This demonstrates the possibility of polarization immunoassays using this high quantum yield rhenium complex. The excitation wavelength was 400 nm and observation was 550 nm with a bandpass of 8 nm, at 20°C.

FIG. 10 shows the chemical structure of [Os(phen)$_2$(aphen)]$^{2+}$ and [Os(tpy)(triphos)]$^{2+}$.

FIG. 11 graphically depicts the absorption spectra of red absorbing osmium probes in acetonitrile at room temperature.

FIG. 12 graphically shows the emission spectra of [Os(phen)$_2$(aphen)]$^{2+}$, [Os(tpy)(triphos)]$^{2+}$, [Os(tppz)$_2$]$^{2+}$, and [Os(ttpy)$_2$]$^{2+}$.

8

FIG. 13 is a graph depicting the anisotropy spectra of $[Os(phen)_2(aphen)]^{2+}$, $[Os(tpy)(triphos)]^{2+}$, $[Os(tppz)_2]^{2+}$, and $[Os(ttpy)_2]^{2+}$ in 9:1 glycerol:methanol at $-55°C$.

5　　　FIG. 14 graphically depicts the intensity decay of long lifetime $[Os(tppz)_2]^{2+}$.

FIG. 15 is an intuitive description of a fluorescence polarization immunoassay. Re-L is $[Re(bcp)(CO)_3(4-COOHPy)]^+$, and θ is the rotational

10　　correlation time.

FIG. 16 graphically shows molecular weight dependent anisotropy for a protein-bound luminophore with luminescence lifetimes of 4, 40, 400, and 2700 ns.

FIG. 17 shows the molecular structures of the

15　　ligands in $[Os(phen)_2(aphen)]^{2+}$, $[Os(tpy)(triphos)]^{2+}$, $[Os(tppz)_2]^{2+}$, and $[Os(ttpy)_2]^{2+}$.

FIG. 18 graphically depicts the absorption spectra of $[Re(bcp)(CO)_3(4-COOHPy)]^+$, 2,9-dimethyl-4,7-diphenyl-1,10-phenanthroline (bcp), and isonicotinic acid (4-

20　　COOHPy) in methanol.

FIG. 19 graphically shows the temperature dependent emission spectra (top) and intensity-normalized emission spectra (bottom) of $[Re(bcp)(CO)_3(4-COOHPy)]^+$ in 100% glycerol. Excitation was 360 nm with

25　　a bandpass of 8 nm.

FIG. 20 depicts the temperature-dependent emission anisotropy of $[Re(bcp)(CO)_3(4-COOHPy)]^+$ in solutions composed of different ratios of glycerol/H_2O (v/v). Emission was monitored at 550 nm with an excitation

30　　wavelength of 400 nm and a bandpass of 8 nm.

FIG. 21 graphically shows excitation spectra and $R(\lambda)$ values for $[Re(bcp)(CO)_3(4-COOHPy)]^+$ in CH_3CN.

FIG. 22 depicts the emission anisotropy spectrum of $[Re(bcp)(CO)_3(4-COOHPy)]^+$ in 100% glycerol at $-60°C$.

9

An emission spectrum is shown for comparison.
Excitation was 400 nm with a bandpass of 8 nm.

FIG. 23 graphically shows the absorption and
emission spectra of [Re(bcp)(CO)$_3$(4-COOHPy)]$^-$ conjugated

5   to HSA in 0.1 M PBS buffer, pH 7.0. Excitation
wavelength was 400 nm. The solid line shows the
excitation anisotropy spectrum in 100% glycerol at -
60°C, with an emission wavelength of 550 nm. The
bandpass was 8 nm for all measurements.

10   FIG. 24 graphically depicts the steady-state
fluorescence polarization of Re-HSA added to
preincubated mixtures of anti-HSA with various
concentrations of unlabeled HSA. The excitation
wavelength was 400 nm and the observation wavelength

15   was 550 nm with a bandpass of 8 nm, at 20°C. Error
bars represent the standard deviations of three
polarization readings.

FIG. 25 shows the absorption spectra of
[Re(bcp)(CO)$_3$(4-COOHPy)]$^+$, 2,9-dimethyl-4,7-diphenyl-

20   1,10-phenanthroline (bcp), and isonicotinic acid (4-
COOHPy) in methanol. The solid line shows the
excitation spectrum of [Re(bcp)(CO)$_3$(4-COOHPy)]$^+$ in
methanol.

FIG. 26 depicts the intensity-normalized emission

25   spectra of free [Re(bcp)(CO)$_3$(4-COOHPy)]$^+$ in CHCl$_3$,
CH$_3$OH, and Re-labeled proteins, Re-HSA and Re-IgG in 0.1
M PBS buffer.

FIG. 27 graphically shows the excitation
anisotropy spectra of free [Re(bcp)(CO)$_3$(4-COOHPy)]$^+$ in

30   100% glycerol and Re-labeled proteins in 60%
glycerol/40% 0.1 M PBS buffer (v/v) with an excitation
band pass of 8 nm, at -60°C.

FIG. 28 depicts the temperature-dependent emission
anisotropy of free [Re(bcp)(CO)$_3$(4-COOHPy)]$^+$ and its

10

protein conjugates in 60% glycerol/40% 0.1 M PBS buffer
(v/v). Excitation wavelength was 400 ± 4 nm; emission
wavelength was 550 ± 4 nm.

FIG. 29 shows the anisotropy decays of free
[Re(bcp)(CO)$_3$(4-COOHPy)]$^+$ at the indicated solutions and
the indicated temperatures.

FIG. 30 graphically shows the anisotropy decays of
Re-labeled proteins in buffer (top) and in the
indicated solutions (bottom).

DETAILED DESCRIPTION OF THE INVENTION

Metal-ligand complexes offer advantages for
optical sensing because they allow lifetime based
sensing with low cost instrumentation. Many of these
complexes display polarized emission. Polarized
emission is valuable because it enables these compounds
to be used for polarization immunoassays.

The metal-ligand complex probes of the invention
have applications in biophysics, clinical chemistry,
and immunoassays. The complexes of the platinum
metals, Ru(II), Os(II), and Re(I), display anisotropy
properties that can be successfully utilized in
fluorescence polarization immunoassays and in studies
of protein and/or lipid hydrodynamics. The complexes
can be comprised of mono, bis, or tris(heteroleptic)
complexes of Ru(II) and Os(II) and carbon monoxide
diimine complexes of Re(I). The metal-ligand complexes
include the high quantum yield rhenium (I) complex of
the formula [Re(bcp)(CO)$_3$(4-COOHPy)]$^+$ and the long
lifetime osmium (II) complexes, [Os(phen)$_2$(aphen)]$^{2+}$,
[Os(tpy)(triphos)]$^{2+}$, [Os(tppz)$_2$]$^{2+}$, and [Os(ttpy)$_2$]$^{2+}$.

The ligands covalently bound to the metals can
include ligands based on diimine, phosphine, arsine,
pyridine, substituted pyridines, carbon monoxide,

11

carbonyl, and any combination thereof. The ligands may
be substituted with functional groups that can be
directly conjugated to macromolecules such as amine
reactive N-hydroxysuccidimide, isothiocyante, sulfonyl

5   chloride containing ligands, sulfhydryl reactive
iodoacetamide, and maleimide containing ligands.

These long lifetime metal-ligand complexes offer
advantages for optical sensing because they allow
lifetime based sensing with low cost instrumentation.

10   These new probes can be used in biophysical chemistry,
immunoassays of high molecular weight antigens, with
red laser diode, red LED, or blue or ultraviolet LED
excitation, and in lifetime immunoassays with improved
spectral properties.

15   [Re(bcp)(CO)$_3$(4-COOHPy)]$^+$ displays a quantum yield
and lifetime considerably longer than that available
with previous metal-ligand complexes. The lifetimes of
[Os(phen)$_2$(aphen)]$^{2+}$, [Os(tpy)(triphos)]$^{2+}$, [Os(tppz)$_2$]$^{2+}$,
and [Os(ttpy)$_2$]$^{2+}$ are longer than that available with

20   previous osmium complexes.

A favorable property of [Re(bcp)(CO)$_3$(4-COOHPy)]$^+$
is that it is not as severely quenched by oxygen in
aqueous solution when bound to biological molecules.
The lifetimes of rhenium labeled DPPG vesicles can

25   exceed 3 μs in oxygenated aqueous solution, and their
quantum yield is 0.2 or larger in oxygenated solutions.
This rhenium (I) complex displays a four fold higher
quantum yield and an eight fold longer lifetime
compared to prior art rhenium (I) complexes. Rhenium

30   labeled HSA is only moderately quenched by dissolved
oxygen, and the average lifetime is near 3 μs.

[Os(phen)$_2$(aphen)]$^{2+}$ and [Os(tpy)(triphos)]$^{2+}$
display a quantum yield of 0.02, which is larger than

12

the quantum yield of previous osmium complexes, in
which the quantum yield was less than 0.001.

The absorption spectra of [Os(phen)$_2$(aphen)]$^{2+}$,
[Os(tpy)(triphos)]$^{2+}$, [Os(tppz)$_2$]$^{2+}$, and [Os(ttpy)$_2$]$^{2+}$

5   extend to 700 nm which allows them to be used with long
wavelength excitation. The emission of these osmium
(II) complexes above 650 nm is desirable for avoiding
autofluorescence from biological samples and for use
with non-invasive transdermal sensing. The high

10   anisotropy of these osmium complexes near 0.3 makes
them useful in fluorescence polarization immunoassays.
It is desirable to have probes which display long
absorption emission wavelengths and also display long
lifetimes. The lifetime of [Os(tppz)$_2$]$^{2+}$ is near 150

15   ns, which is 10-fold larger than obtained with prior
art osmium (II) complexes, which displayed a lifetime
of 14 ns. The long lifetime permits such probes to be
used with gated detection to avoid interfering
autofluorescence.

20   Luminescence probes have high sensitivity and
specificity. Luminescence probes based on metal-ligand
complexes are valuable in biochemistry and biophysics.

The invention is applicable to long-lived, highly
luminescent rhenium (I) metal-ligand complexes as

25   biomolecular probes.
The newly synthesized rhenium(I) metal-ligand
complex [Re(bcp)(CO)$_3$(4-COOHPy)],where bcp is 2,9-
dimethyl-4,7-diphenyl-1,10-phenanthroline and 4-COOHPy
is isonicotinic acid, exhibits high quantum yields,

30   long lifetimes, and high anisotropy in the absence of
rotational diffusion, and can be conjugated to proteins
and lipids.

13

The flexibility in selection of the metal and the ligand renders metal-ligand complexes a versatile class of biomolecular probes. A wide range of lifetimes, absorption and emission spectra, and polarization

5   characteristics offers numerous experimental opportunities in biophysics and clinical chemistry. For instance, a long lifetime is desirable for fluorescence polarization immunoassays of high-molecular-weight antigens, whereas a long wavelength is

10 favorable for non-invasive clinical applications, due to lower autofluorescence and higher tissue transmission at longer wavelengths.

With its high quantum yields, long lifetimes, as well as its highly polarized emission, this rhenium (I)

15 complex may expand the measurement of rotational motions to timescales > 10 µs when bound to macromolecules.

The use of such metal-ligand complexes enable fluorescence polarization immunoassays to bypass the

20 usual limitation to low-molecular-weight antigens. The usual limitation is a consequence of the < 10 ns decay times of the previously used fluorophores.

The invention is also applicable to fluorescence polarization immunoassays of high molecular weight

25 analytes.

A new FPI probe, [Re(bcp)(CO)$_3$(4-COOHPy)](ClO$_4$), for high molecular weight antigens has been synthesized. This Re(I) complex displays highly polarized emission (with a maximum polarization near

30 0.4 and maximum anisotropy near 0.3) in the absence of rotational diffusion and a long average lifetime (2.7 µs) when bound to proteins in air-equilibrated aqueous solution. The steady-state polarization of the Re(I)

14

complex labeled HSA conjugate (Re-HSA) was sensitive
to the binding of anti-HSA, resulting in a significant
increase in luminescence polarization. The labeled HSA
was also used in a competitive format with unlabeled

5   HSA acting as an antigen. More importantly, the
lifetime of this probe when covalently labeled to HSA
in air-equilibrated aqueous solution is near 3 μs,
which theoretically allows immunoassays of antigens
with molecular weights up to 10^8 Daltons (Figure 16).

10   The fluorescence polarization (P) of a labeled
macromolecule depends on the fluorescence lifetime (τ)
and the rotational correlation time (θ):

15

$$\left|\frac{1}{P}-\frac{1}{3}\right|=\left|\frac{1}{P_0}-\frac{1}{3}\right|\left(1+\frac{\tau}{\theta}\right) \tag{1}$$

where P_0 is the polarization observed in the absence of rotational diffusion. The effect of molecular weight on the polarization values can be seen from an
5   alternative form of Equation 1:

$$\left(\frac{1}{P}-\frac{1}{3}\right)=\left(\frac{1}{P_0}-\frac{1}{3}\right)\left(1+\frac{kT}{\eta V}\tau\right) \tag{2}$$

where k is the Boltzmann constant, T is the absolute temperature in Kelvin, η is the viscosity of the solution, and V is the molecular volume. The molecular
10   volume of the protein is related to the molecular weight (M_r) and the rotational correlation time by:

$$\theta=\frac{\eta V}{kT}=\frac{\eta M_r}{RT}(\overline{v}+h) \tag{3}$$

where R is the ideal gas constant, $\overline{v}$
15   is the specific volume of the protein, and h is the hydration, typically 0.2 g $H_2O/1$ g protein. Generally, the observed correlation times are about twofold longer than those calculated for an anhydrous sphere (Eq. 3 with $h=0$) due to the effects of hydration and the
20   nonspherical shapes of most proteins. Therefore, in aqueous solution at 20°C ($\eta=1cP$), one can expect a protein such as HSA ($M_r \sim 65,000$ Da, with $\overline{v} + h = 1.9$) to display a rotational correlation time near 50 ns.

16

The advantage of using a luminophore with a long
lifetime is illustrated by comparing the expected
polarization values for materials with different
molecular weights, labeled with probes with different

5   lifetimes, Figure 16. It is convenient to use the
anisotropy (r) in this calculation. The anisotropy and
polarization are related by:

$$P = \frac{I_\| - I_\perp}{I_\| + I_\perp} \qquad (4)$$

$$r = \frac{I_\| - I_\perp}{I_\| + 2 I_\perp} \qquad (5)$$

10   where $I_\|$ and $I_\perp$ are the vertically and horizontally
polarized components of the emission. The values of P
and r can be interchanged using:

$$r = \frac{2P}{3 - P} \qquad (6)$$

$$P = \frac{3r}{2 + r} \qquad (7)$$

15   The parameters P and r are both commonly used to
describe rotational diffusion processes of fluorophores
in solution. The values of P are more often used in
FPI because they are entrenched by tradition and are
slightly larger than the anisotropy values. The

20   parameter r is preferred on the basis of theory. The
anisotropy of a labeled macromolecule is:

17

$$r = \frac{r_0}{1 + \tau/\theta} \qquad (8)$$

where r_0 is the anisotropy in the absence of rotational diffusion and is typically near 0.3 for most fluorophores, although the theoretical limit given

5   colinear transition dipoles for absorption and emission is 0.4.

The expected anisotropy values for a range of photoluminescence lifetimes were simulated. These calculations were based on Equations 3 and 8,

10    $\overline{v}$ established on the assumptions that the limiting anisotropy $(r_\circ)$ was 0.3 in the absence of rotational diffusion, the solution viscosity was 1 cP, and + h = 1.9 for the protein. These simulations demonstrate how the lifetime of the luminophore

15   determines the range of molecular weights which can be resolved by the luminophore in an immunoassay. Presently, most immunoassays rely on fluorescein and rhodamine derivatives as fluorescent probes ($\tau \sim$ 4 ns). If one considers that most low molecular weight

20   antigens are in the range of < 1000 Da, the expected anisotropy of the labeled antigen can be estimated from Figure 16 to be in the range of 0.05. Upon antigen association with antibody, the molecular weight increases ($Mr \sim$ 160,000 Da) and the anisotropy of the

25   bioconjugate approaches 0.30. Hence, a large change in anisotropy is found upon binding of Ag to Ab for low molecular weight antigens, when utilizing a 4 ns lifetime fluorophore.

However, if the molecular weight of the labeled

30   antigen is larger, above 20,000 Da, then the anisotropy changes only slightly upon binding to antibody, if the

18

same fluorophore is used. For instance, suppose the
molecular weight of the labeled antigen is 160,000 Da,
with a rotational correlation time of 125 ns., and that
of the antibody-bound form is 600,000 Da, with a

5   rotational correlation time of 470 ns. In this
particular case, the anisotropy values will differ by
less than 2% between the two forms using a short
lifetime fluorophore. This small change is attributed
to the large discrepancy between the lifetime of the

10   fluorophore and the rotational correlation time of the
labeled macromolecular complex. It is this reason why
FPI's are performed only in the low molecular weight
range with conventional short lifetime fluorophores.

The lifetime of the luminophore $[Re(bcp)(CO)_3(4-$
15      $COOHPy)]^-$ is in the range of 3 µs. For the example
described above, the binding assay would now be
detectable using luminescence polarization (Figure 16).
Theoretically, a luminophore with a lifetime of 3 µs
could allow the analysis of biological systems with

20   molecular weights up to 100 million Daltons and
correlation times up to 80 µs, thereby greatly
expanding the capabilities of FPI's to include the
study of entire cells, viruses, and other large
biomolecules and biomolecular complexes.

25   The superior approach for the direct measurement
of high molecular weight analytes in an immunoassay is
to develop luminescence probes with lifetimes that are
comparable to the rotational correlation times of the
antibody, antigen, and the bioconjugates they form.

30   The use of the photoluminescence from metal-to-ligand
charge transfer (MLCT) excited states in this regard is
definitely the proper direction of this research. The
sensitivity and dynamic range of a generic immunoassay
can be correlated well to the lifetime of the probe

19

used and the hydrodynamic volumes (molecular weight) of the bound and free tracer antigen (Figure 16). To observe comparable anisotropy values for a 2.7 μs probe as that of a 4 ns probe, the molecular weight range can

5   be at least 3 orders of magnitude larger in the former case.

Two disadvantages of MLCT complexes are their low extinction coefficients and quantum yields when compared to a probe like fluorescein. The extinction

10 coefficients of MLCT compounds are generally 2-5 fold lower than fluorescein. There is generally about a 10-fold difference in quantum yield between fluorescein and MLCT compounds. However, these disadvantages are offset by the fact that the photostability of MLCT

15 complexes is remarkable compared to fluorescein, and MLCT compounds do not display any probe-probe interactions, quite unlike fluorescein, which allows for a much larger dye:protein ratio when labeling with MLCT complexes. In addition, the long-lifetimes of

20 MLCT complexes allow for the off-gating of the autofluorescence from biological samples which takes place in the 1-10 ns timescale, which is not possible with fluorescein.

MLCT probes display lifetimes that range from sub-

25 nanosecond to >100 μs. Therefore, MLCT compounds can be specifically tailored to be used in any immunoassay. MLCT compounds can be systematically engineered to alter their spectroscopic, photophysical, and chemical properties. The spectral and chemical versatility of

30 MLCT complexes allows the design of probes displaying lifetimes that respond to specific molecular weights. Compared to $[Ru(bpy)_2(dcb)]^{2+}$, $[Re(bcp)(CO)_3(4-COOHPy)]^+$ displays higher quantum yield, higher anisotropy, and longer lifetime. The quantum yields of

20

[Ru(bpy)$_2$(dcb)]$^{2+}$ and [Re(bcp)(CO)$_3$(4-COOHPy)]$^+$ are about 0.05 and 0.12, respectively, when bound to protein.

The invention is applicable to anisotropy probes for protein hydrodynamics.

5   The newly made Re-complex, [Re(bcp)(CO)$_3$(4-COOHPy)](ClO$_4$), can be used as an anisotropy probe for protein hydrodynamics. [Re(bcp)(CO)$_3$(4-COOHPy)]$^+$ displays highly polarized emission with a maximal anisotropy near 0.3 in frozen solution, thus making it

10   useful as an anisotropy probe. [Re(bcp)(CO)$_3$(4-COOHPy)]$^+$ was conjugated to human serum albumin (HSA) and bovine immunoglobin G (IgG). Long excited-state lifetimes in fluid solutions equilibrated with air at room temperature were found for [Re(bcp)(CO)$_3$(4-

15   COOHPy)]$^+$ when covalently linked to HSA and IgG. Analyses of the anisotropy decays of the protein conjugates demonstrate that [Re(bcp)(CO)$_3$(4-COOHPy)]$^+$ can be used to measure rotational motions on the 10 ns to ~100 μs timescale in air equilibrated solutions.

20   [Re(bcp)(CO)$_3$(4-COOHPy)]$^+$ can be used as an anisotropy probe for macromolecular dynamics. The anisotropy decays are dependent on protein dynamics. The correlation time has been extended to 100 μs, which has been inaccessible with routinely used nanosecond

25   probes. This metal-ligand complex, with its high quantum yield, long lifetime, and highly polarized emission has opened a new timescale regime for the study of macromolecular dynamics.

The usefulness of the fluorescence anisotropy

30   measurements is derived from its dependence on the extent of rotational diffusion during the lifetime of the excited state. Two basic kinds of information my be derived from fluorescence anisotropy decay

21

measurements. Anisotropy decay may provide information
as to the size and shape factor of macromolecules,
reflecting the macromolecule and the attached
fluorophore which rotate as a unit. Anisotropy decays
5   may also provide information about the internal
rotational motions present in the macromolecules and
the nature of the molecular flexibility. Information
about the rotational motion is available over a time
range extending to about 3 times the fluorescence
10   lifetime, after which there is too little signal for
accurate anisotropy measurements. Because the lifetime
of typical fluorophores ranges from 1 to 10 ns, it is
difficult to measure rotation correlation times larger
than 30 ns. Therefore, it is difficult to determine
15   the rotational hydrodynamics of larger proteins or
membrane-bound proteins.

The invention also is applicable to red
fluorescent dyes for biophysics and for sensors.
Several polypyridine compounds of osmium(II) have
20   been synthesized. These compounds can be conjugatable
to proteins, typically absorb above 550 nm, emit above
700 nm and their lifetimes are higher than 50 ns. The
emission of these compounds is polarized, so they have
excellent applications as LED excitable and red
25   emitting dyes for biophysical experiments. The low
energy absorption as well as emission and high lifetime
can be used for lifetime based oxygen sensing.
We have developed rhenium and osmium metal ligand
complexes which are very photostable, have polarized
30   emission and long decay times. The longer decay times
allow increased sensitivity using gated detection
following decay of the unwanted autofluorescence. Some
lanthanide chelates compounds show longer decay times

22

which allow gated detection and increased sensitivity for immunoassays, but do not display polarized emission, which is required for protein hydrodynamics.

5 The dyes consist of MLCT complexes of osmium(II) metal with polypyridine and nonchromophoric tridentate phosphine ligands. Figure 17 represents the structure of all ligands used, and Figure 10 represents the structure of two complexes of each class. All these complexes show good fundamental anisotropy (r_0) and long

10 decay times. Therefore, they can be used in biophysics to study the hydrodynamics of macromolecules. Another added advantage of using these complexes is their high photo-stability in solvents.

The long lifetimes of rhenium (I), ruthenium (II)

15 and osmium (II) complexes allow their use as oxygen sensors. The effect of oxygen on osmium complexes is less than its effect on the analogous ruthenium complexes because of shorter excited state lifetimes. The lifetime of these complexes is long enough to use

20 them as oxygen sensors for lifetime based sensing using low-cost phase fluorometry with red emitting, LED light sources. The effect of oxygen on $[Os(tppz)_2]^{2+}$ is represented in Figure 14.

Because of their long decay lifetimes, diode laser

25 excitability (absorb at 500 -700 nm), low energy emission (emit in red region, 700-750 nm), reasonable quantum yields, polarized emission (anisotropy 0.15-0.35) and high photo-stability, these osmium(II) polpyridine complexes can be used as fluorophores in

30 biophysical applications. These complexes can be used as red fluorophores for macromolecules. When using these fluorophores, one can avoid low signal to noise level by using gated observation. Another advantage of

23

these compounds is high photostability. These dyes can
be handled in room light for months.

These metal ligand complexes can be prepared with
different functional groups for conjugation to

5   biological macromolecules. These include
isothiocyanate, sulfonyl chlorides, iodoacetamides, and
malimides. Also, the organic ligands bound to the
rhenium and osmium atoms can be varied to further
modify the absorption and emission spectral properties.

10   The invention is further illustrated by the
following examples, which are not intended to be
limiting.

Example 1:
A Long-Lived, Highly Luminescent Rhenium (I) Metal-

15   Ligand Complex As A Biomolecular Probe
Human serum albumin (HSA), bovine immunoglobulin G
(IgG), dipalmitoyl-L-α-phosphatidylethanolamine (PE)
and dipalmitoyl-L-α-phosphatidylglycerol (DPPG) were
obtained from Sigma Chemical Co. and were used without

20   further purification. 2,9-dimethyl-4,7-diphenyl-1,10-
phenanthroline (bcp), isonicotinic acid (4-COOHPy),
$AgClO_4$, NH_4PF_6, and $Re(CO)_5Cl$ were obtained from Aldrich
and used as received. The other solvents used were of
HPLC or spectroscopic reagent grade. FTIR spectra were

25   obtained on a Perkin Elmer 1600 Series
spectrophotometer with 4 cm-1 resolution. Samples were
dissolved in dichloromethane and measured in a liquid
cell.

24

Re(bcp)(CO₂)₃Cl Synthesis

Re(CO)₅Cl (1 g, 2.76 mmol) was reacted with bcp(1.05 g, 2.9 mmol) in toluene under reflux with stirring for 1 hour. The solution was cooled to room

5   temperature and hexane was added which precipitated a yellow solid. This was collected on a coarse frit and washed with toluene followed by hexane. The product was dried under vacuum. Yield: 1.52 g (83%). Anal. Calcd for $ReC_{29}H_{20}N_2O_2Cl$: C, 52.29; H, 3.03; N, 4.21.

10   Found: C, 52.04; H, 2.93; N, 3.95. IR (νCO: 2021(vs), 1914(vs), 1895(vs) cm^{-1}).

Re(bcp)(CO₃)(PyCOOH) Synthesis

Re(bcp)(CO)₃Cl (1.5 g, 2.25 mmol), $AgClO_4$ (514 mgs, 2.48 mmol), and 4-COOHPy (8.3 g, 67.5 mmol) were

15   refluxed in 4:1 MeOH:toluene under argon in the dark for 24 hours. This was cooled to room temperature and filtered to remove the AgCl precipitate. The filtrate was rotovaped to dryness and the solid resuspended in CH_2Cl_2 and filtered (to remove 4-COOHPy). The filtrate

20   was rotovaped to dryness and a bright yellow solid was obtained. Yield: 1.8 g (94 %). Anal. Calcd for $ReC_{35}H_{25}N_3O_9Cl$: C, 49.27; H, 2.95; N, 4.92. Found: C, 50.30; H, 2.98; N, 4.80. IR (νCO: 2034(vs), 2022(vs), 1919(vs) cm^{-1}). FAB-MS[M-ClO₄$^-$]:755. The

25   hexafluorophosphate salt was prepared by methathesis of the perchlorate salt by dissolving it in 1:1 acetone:H_2O and precipitating it by the addition of a concentrated aqueous solution of NH_4PF_6. High purity luminescence samples were prepared using chromatography procedures

30   previously described in the literature. (Wallace, L., and Rillema, D.P. (1993) *Inorg. Chem.* 32, 3836-3843; Sacksteder, L., Zipp, A.P., Brown, E.A., Streich, J.

25

Demas, J.N., and DeGraff, B.A. (1990) *Inorg. Chem.* 29, 4335-4340).

Preparation of Activated Succimidyl Ester

5 mg of N,N'-dicyclohexylcarbodiimide (DCC) and 3
5   mg of N-hydroxy-succinimide (NHS) were dissolved in
        0.15 ml of DMF with stirring, 10 mg of the Re-complex
        in 0.15 ml of DMF was then added, and the mixture was
        stirred for a few hours. The formed precipitate was
        removed by filtration through a syringe filter, and the
10   filtrate containing the active Re-complex was used for
        labeling the substrates.

        The proteins HSA and IgG (10 mg of protein) were
        labeled by adding a 15-fold molar excess of the Re-NHS
        in 50 µl of DMF to 1 ml of stirred protein solution
15   (0.2 M carbonate buffer, pH 8.5), followed by a 5 h
        incubation and purification of the labeled protein by
        gel filtration chromatography on Sephadex G-25, using
        0.1 M PBS, pH 7.0. Our 0.1 M PBS (phosphate buffered
        saline) consisted of 0.1 M NaH_2PO_4 and 0.1 M $NaHPO_4$ in
20   deionized water. The dye:protein ratio of the Re-HSA
        conjugate was determined to be 2:1. The concentration
        of the protein was determined by the Coomassie Plus
        Protein Assay (Pierce) and the concentration of the
        Re(I) complex was determined by its absorbance at 400
25   nm (e = 5040 $M^{-1}cm^{-1}$), assuming the same extinction
        coefficient as the free complex.

        95 mg of the Re-complex and 13 mg of NHS were
        dissolved in 0.7 ml of $CHCl_3$ at room temperature, 24 mg
        of DCC was then added. The mixture was sealed and
30   stirred for a few hours. The formed precipitate was
        removed by filtration through a syringe filter, and the
        filtrate containing the active Re-complex was slowly
        added to a stirred solution of PE (60 mg in 7.5 ml of

26

CHCl₃) and triethylamine (4.5 ml) under an argon
atmosphere. The mixture was stirred for 20 h in the
dark. The solvents were removed under vacuum and the
product was redissolved in 1.0 ml of CHCl₃/MeOH

5   (1/1,v/v). The pure Re-PE was obtained by TLC on K6F
silica gel plates using CHCl₃/CH₃OH/NH₃OH (65/25/4,
v/v/v) as the developing solvent. The R_f value of the
product is about 0.91, relative to that of PE (0.55).

For vesicle preparation, lipids with a Re-

10   lipid/DPPG mole ratio of 1:200 were dissolved in CHCl₃,
and the solvent was removed by a stream of argon.
Vesicles were prepared by sonicating in 10 mM Tris, 50
mM KCl, pH 7.5, at a final lipid concentration of 2
mg/ml of DPPG. The DPPG vesicles in the absence of Re-

15   lipid did not display significant emission signals (< 2
%) under the present experimental conditions. Before
sonication, the lipid and Re-complex were vacuum
dessicated overnight to remove any traces of organic
solvent. The vesicle solutions were deoxygenated by

20   bubbling argon for 20 minutes, followed by
equilibration with an argon atmosphere for 20 minutes,
and then a subsequent 20 minute bubbling of the
solution with argon.

Emission spectra were recorded on a SLM AB-2

25   spectrofluorimeter. The frequency-domain
instrumentation (ISS) was used for measurements of
luminescence intensity decays. The frequency-domain
lifetime measurements of the free dye in solution were
performed on an ISS (Champaign, IL) K2 fluorimeter,

30   using a Panasonic high intensity blue LED (light-
emitting diode) configured to provide amplitude
modulated light centered at 390 nm. (Sipior, J.,
Carter, G.M., Lakowicz, J.R., and Rao, G. (1997) *Rev.
Sci. Instrum.* 68(7), 2666-2670). An Andover (Salem,

27

NH) 500 nm long-wave pass filter (500FH90-50S) was used to isolate the emission. For DPPG vesicle samples, frequency-domain lifetime measurements were performed using a Xenon arc lamp (300W) as the light source. The

5   excitation was amplitude modulated by an electro-optical low-frequency modulator (K2.LF from ISS) using 340 ± 8 nm as the excitation wavelength. A 470 nm long-pass filter (Corning 3-71) was used to isolate the emission.

10   The frequency-domain intensity data were fitted by a nonlinear least squares procedure and were modeled with single and multi-exponential decay laws. The intensity decays were described by

$$I(t) = \sum_i \alpha_i e^{-t/\tau_i}$$

15   (9)

where $I(t)$ is the luminescence intensity at time t, α_i and τ_i are the pre-exponential weighting factors and the excited-state lifetimes, respectively. The subscripts denote individual components. Mean lifetimes were

20   calculated using Equation 9.

$$\langle \tau \rangle = \sum_i \alpha_i \tau_i^2 / \sum_i \alpha_i \tau_i \qquad (10)$$

The measured excitation anisotropy spectra are defined by Equation 5, where $I_\parallel$ and $I_\perp$ are the emission intensities measured with vertically polarized

25   excitation and the emission polarization parallel ($I_\parallel$) or perpendicular ($I_\perp$) to the excitation. The values of the polarized intensities were corrected for the

28

transmission efficiency of the polarized components by
the detection optics.

    As a probe of emission heterogeneity, the
excitation spectra method described by Demas and co-

5   workers (Sacksteder, L., Demas, J.N., and DeGraff, B.A.
(1989) *Inorg. Chem.* 28, 1787-1792) was used. In brief,
two uncorrected excitation spectra were measured with
different emission wavelengths (λ_1 and λ_2). R (λ) is
calculated as

10                    $$R\ (\lambda)\ =\ E_1\ (\lambda)\ /\ E_2\ (\lambda) \qquad\qquad (11)$$

where the *E's* are the emission intensities while
exciting at λ and monitoring at two different
wavelengths, λ_1 and λ_2. Since the sample absorbance and
excitation intensities are the same at each excitation

15   wavelength, R is related to the relative contributions
of different emission components. If there is no
ground-state heterogeneity or the equilibration in the
excited state is rapid relative to sample decay times,
R (λ) is wavelength independent. If there are multiple

20   ground-state species that fail to equilibrate in their
excited states, R (λ) varies with λ.

    The molecular structure of [Re(bcp)(CO)$_3$(4-
COOHPy)]$^+$ is shown in Figure 1. The absorption spectrum
of the Re-complex in CH_3OH is shown in Figure 18. The

25   absorption spectra of the ligands in CH_3OH are also
shown for comparison. The spectra are normalized to
unity to facilitate comparison. The maximum of the
low-energy absorption band around 340 ~ 450 nm and the
more intense higher energy absorption at 298 nm are the

30   characteristic MLCT and π-π* bands, respectively. It

29

is important to note that this complex can be excited
with the UV output of a blue light emitting diode.

The excitation and emission spectra of the Re
complex in $CHCl_3$, CH_3OH and CH_3CN are shown in Figure 2.

5   The large Stokes' shift of this Re complex (~100 nm)
makes it a good candidate for energy transfer studies
as there is no possibility for self-quenching. Also,
the large Stokes' shift indicates a macromolecule can
be labeled with multiple MLCT without self-quenching.

10   This emission of this complex displays a strong
sensitivity to local environment, as observed from the
spectral shift of 539 nm in $CHCl_3$ to 559 nm in 0.1 M PBS
buffer solution at room temperature. When bound to
biomolecules it is reasonable to expect that this

15   complex's emission may respond to the subtle changes in
the micro-environment of a biological sample. The
emission intensity is strongly dependent on temperature
as shown by the increased intensity at -57 °C compared
with 19 °C (Figure 19). There is also a significant

20   blue-shift in emission maximum with decreasing
temperature (Figure 19). These results are consistent
with the temperature dependence of many other MLCT
complexes, wherein the energy gap between the ground
and excited states increases with decreasing

25   temperature resulting in a blue-shifted emission
spectrum, increased lifetime, and higher quantum yield.

The lifetimes and quantum yields for
$[Re(bcp)(CO)_3(4-COOHPy)]^+$ are summarized in Table 1.

30

Table 1. Photoluminescence quantum yields and
lifetimes of Re(bcp)(CO)$_3$(4-COOHPy)(PF$_6$) at room
temperature unless otherwise indicated.

Solvent	Conditions	φ[a]	τ(µs)	mean τ(µs)
CH$_3$OH	Air	0.039	0.54	
	Argon	0.54	7.25	
CHCl$_3$	Air	0.047	0.66	
	Argon	0.55	6.72	
CH$_3$CN	Air	0.016	0.49	
	Argon	0.23	4.65	
Glycerol	Air	0.27	10.8	
Re-PE in DPPG vesicles	Air	0.13 (22°C)		4.36(2°C) 3.31(10°C) 2.54(22°C) 1.99(35°C) 1.82(50°C)
	Argon	0.27		
Re-IgG	Air	0.12		2.92
	Argon	0.22		4.07
Re-HSA	Air	0.20		2.75
	Argon			3.44
0.1 M PBS	Air		0.99	

[a] Absolute quantum yields are difficult to determine in
the presence of uncertain amounts of dissolved oxygen
under air-equilibrated conditions.

Demas and co-workers have demonstrated that certain
rhenium complexes display high quantum yields, in
excess of 0.7, and long lifetimes in excess of 10 µs
in fluid solutions at room temperature. (Sacksteder,
L., Lee, M., Demas, J.N., and DeGraff, B.A. (1993) *J.
Am. Chem. Soc.* 115, 8230-8238). Our novel Re(I)
complex is a remarkable example of such a high quantum
yield long lifetime probe. It displays a lifetime over
10 µs in air-equilibrated glycerol, and long lifetimes

31

when the lipid conjugate Re-PE is embedded in DPPG
model vesicles, as shown in Table 1. Owing to its long
lifetime, it is also extremely sensitive to oxygen
quenching.   There is a significant increase in
5   intensity with the removal of oxygen from the solution,
as shown in Figure 3. In methanol, in the absence of
oxygen, a homogeneous intensity decay with a lifetime
of 7248 ns was found. In the presence of dissolved
oxygen, from equilibrium with air, the lifetime reduced
10   to 538 ns (Figure 4). This result suggests that this
complex may be used as an oxygen sensor under certain
circumstances. The oxygen quenching, however, is much
less efficient when the probe is bound to
macromolecules, such as phospholipid vesicles, than
15   when free in solvents (Figure 5). We attribute this to
a shielding of the excited state from oxygen quenching
by macromolecules. More importantly, this complex
displays a lifetime of 2.54 μs and a quantum yield of
0.13 in DPPG vesicles in aqueous solution at 22 °C,
20   which indicates that this long-lived probe can be used
in presence of dissolved oxygen and still display a
long decay time and exhibit a high quantum yield.

        We also studied the polarized emission of this
complex in the absence of rotational diffusion
25   (glycerol, -60°C). The excitation anisotropy spectrum
is shown in Figure 2 which displays a maximum
anisotropy near 0.3 from 390 nm to 450 nm. The
anisotropy of this complex is also sensitive to
solution viscosity, as shown in Figure 20. Figure 20
30   is not meant to yield an exact relationship between the
anisotropy and solution viscosity. For example, at the
same temperature, the viscosity of a 100% glycerol
solution is larger than that of a 60% glycerol:water

32

solution, and the anisotropy values demonstrate this behavior.

Rhenium (I) complexes are known to display dual emission, which can originate from either a metal-to-ligand charge transfer state or a ligand-centered state (LC). The MLCT states typically show an unstructured emission whereas the LC states often display a structural emission which is characteristic of ligand. The emission spectra in Figure 2 are unstructured, suggesting that under our experimental conditions the emission is from a pure MLCT state. The $R(\lambda)$ values are flat across the excitation spectrum, which suggests that regardless of excitation wavelength, only one excited state parentage is created (Figure 21).

To further clarify the nature of the emission, and to characterize this complex for use as biophysical probe, we examined the emission anisotropy (Figure 22). The anisotropy is rather constant across the entire emission spectrum and displays a gradual decrease with increasing wavelength.

For use as a biomolecular probe, this complex was used to label the proteins bovine IgG and HSA, as well as the lipid PE. The lipid conjugate Re-PE was used to label the DPPG vesicles. The preliminary results demonstrate that this complex is conjugatable and that its water solubility is adequate for the usual labeling procedures used with the biomolecules. The typical frequency-domain intensity decays of DPPG vesicles labeled with Re-PE are shown in Figure 6. The decays were best fit using three exponential components, along with a scattering component. The recovered long lifetimes when bound to proteins and lipid model vesicles indicate that this complex might be used to

33

study protein and membrane hydrodynamics and measure
rotational correlation times longer than 10 µs.

Example 2:

Fluorescence Polarization Immunoassays of High
5   *Molecular Weight Analytes*

Human serum albumin (HSA), human immunoglobulin G
(IgG), and monoclonal IgG specific for HSA (anti-HSA)
from mouse ascites were obtained from Sigma Chemical
Co. and were used without further purification. All
10   other reagents and all solvents used were reagent
grade. The synthesis of [Re(bcp)(CO)$_3$(4-COOHPy)](ClO$_4$)
is described in Example 1.

5 mg of N,N'-dicyclohexylcarbodiimide (DCC) and 3
mg of N-hydroxy-succinimide (NHS) were dissolved in
15   0.15 mL of DMF with stirring. [Re(bcp)(CO)$_3$(4-
COOHPy)](ClO$_4$) (10 mg in 0.15 mL of DMF) was added, and
the mixture was stirred for 20 hours. The formed
precipitate was removed by filtration through a syringe
filter, and the filtrate containing the activated Re-
20   complex was used for labeling the substrates.

The protein HSA (10 mg) was labeled by adding a
15-fold molar excess of the activated Re-complex in 50
µl of DMF to 1 mL of stirring protein solution (0.2 M
carbonate buffer, pH 8.5), followed by a 5 hr
25   incubation. The conjugate was purified by gel
filtration chromatography on Sephadex G-25, using 0.1 M
PBS, pH 7.0 as eluent. The dye:protein ratio of the
Re-HSA conjugate was determined to be 2:1. The
concentration of the protein was determined by the
30   Coomassie Plus Protein Assay. The concentration of the
Re(I) complex was determined by its absorbance at 400
nm, assuming the extinction coefficient was the same as

34

that of the free dye (ε_{400} = 5040 $M^{-1}cm^{-1}$). (Guo, S.Q.,
Li, L., Castellano, F.N., Szmacinski, H., Lakowicz,
J.R. *Anal. Biochem.* submitted). The equilibrium
association constants of the bioconjugates were
5   determined from luminescence anisotropy data as
described in the literature. (Dandliker, W.B., Kelly,
R.J., Dandliker, J., Farquhar, J., Levin, J.
Immunochemistry 1973, 10, 219-227).

Uncorrected emission spectra were recorded on a
10 SLM AB2 Spectrofluorimeter. The frequency-domain
lifetime measurements were performed on an ISS K2
fluorimeter, using a high intensity Panasonic blue LED
(light-emitting diode) configured to provide amplitude
modulated light centered at 390 nm. (Guo, X.Q., Li,
15 L., Castellano, F.N., Szmacinski, H., Lakowicz, J.R.
Anal. Biochem. Submitted; Sipior, J., Carter, G.M.,
Lakowicz, J.R., Rao, G. *Rev. Sci. Instrum.* 1997, 68(7),
1-5). An Andover 500 nm long pass filter (500FH90-50S)
was used to isolate the emission.

20   The frequency-domain intensity decay data were fit
by a nonlinear least squares procedure, generally to a
sum of three single-exponential decays. The intensity
decays were described by Equation 9. Mean lifetimes
were calculated using Equation 10.

25   The excitation anisotropy spectrum is defined by
Equation 5, where $I_{\parallel}$ and $I_{\perp}$ are the emission intensities
measured with vertically polarized excitation and the
emission polarization parallel ($I_{\parallel}$) or perpendicular
($I_{\perp}$) to the excitation. The values of the polarized
30 intensities were corrected for the transmission
efficiency of the polarized components by the detection
optics.

35

The molecular structure of [Re(bcp)(CO)$_3$(4-COOHPy)]$^+$ is shown in Figure 1. The absorption and emission spectra of [Re(bcp)(CO)$_3$(4-COOHPy)]$^-$ labeled to HSA are shown in Figure 23. The spectra are normalized

5 to unity for comparative purposes. The absorption profile in the low-energy region (340-425 nm) and the more intense higher energy band at 290 nm are characteristic metal-to-ligand charge transfer and π - π* transitions, respectively. The emission spectrum is

10 broad and has a maximum near 550 nm. These photophysical characteristics are similar to that observed with the parent complex [Re(bcp)(CO)$_3$(Py)]$^+$, where Py is pyridine. (Zipp, A.P., Sacksteder, L.A., Streich, J., Cook, A., Demas, J.N., DeGraff, B.A.

15 *Inorg. Chem.* 1993, 32, 5629-5632). The large Stokes' shift of MLCT complexes in general can be exploited in biological media where multiple labeling of close proximity residues will not result in self-quenching processes.

20 O$_2$ quenching is commonplace from MLCT excited states of Re(I) complexes. (Guo, X.Q., Li, L., Castellano, F.N., Szmacinski, H., Lakowicz, J.R. *Anal. Biochem.* Submitted; Sacksteder, L.A., Zipp, A.P., Brown, E.A., Streich, J., Demas, J.N., DeGraff, B.A.

25 *Inorg. Chem.* 1990, 29, 4335-4340; Zipp, A.P., Sacksteder, L.A., Streich, J., Cook, A., Demas, J.N., DeGraff, B.A. *Inorg. Chem.* 1993, 32, 5629-5632). In the case of [Re(bcp)(CO)$_3$(4-COOHPy)]$^+$, the oxygen quenching is modest when the probe is bound to HSA in

30 air-equilibrated aqueous solution. Compared to a deoxygenated buffer solution (1.0), the relative photoluminescence intensity of Re-HSA in air-equilibrated buffer solution is 0.69 (Figure 7).

36

We examined the steady-state excitation anisotropy
spectrum of [Re(bcp)(CO)₃(4-COOHPy)]⁺ in vitrified
solution (glycerol, -60°C) where rotational diffusion
does not occur during the excited state lifetime

5   (Figure 23). This complex shows a maximum anisotropy·
near 0.3, whose values are constant from 390 nm to 450
nm.

Frequency-domain intensity decays of Re-HSA in
air-equilibrated and argon-equilibrated 0.1 M PBS

10   buffer solutions are shown in Figure 8. The analysis
of the frequency-domain intensity decays are summarized
in Table 2.

Table 2. Recovered intensity decays parameters of
[Re(bcp)(CO)₃(4-COOHPy)]⁺ conjugated to HSA.

	Condition	τ_i (µs)	α_i	Mean τ (µs)
Re-HSA	Air	5.76	0.02	
		1.27	0.13	
		0.053	0.85	2.75
	Argon	6.23	0.03	
		1.39	0.11	
		0.051	0.87	3.44

The decays were best fit to a sum of three-exponential
decay laws. The mean lifetimes are 2.75 µs in air-
equilibrated and 3.44 µs in argon-equilibrated buffer

20   solutions, respectively. The elimination of oxygen is
therefore not required for use in fluorescence
polarization immunoassays of high molecular weight
analytes.

37

To evaluate the feasibility of using
[Re(bcp)(CO)$_3$(4-COOHPy)]' in a polarization immunoassay,
Re-HSA was used as an antigen. We examined the changes
in anisotropy of Re-labeled HSA in the presence of

5   increasing amounts of anti-HSA. The polarization
increased about four-fold from 0.023 to 0.108 which
corresponds to anisotropy values ranging between 0.017
to 0.075 (Figure 9). Similar results were obtained
using two different batches of anti-HSA with antibody

10   (Ab) concentrations ranging from 0 to 8 times that of
Re-HSA (Ag). An association constant was calculated
from the data in Figure 9 and found to be 3.3 μM^{-1}. We
used nonspecific human IgG as a control, and no
detectable changes in polarization of Re-HSA were

15   observed in that experiment (Figure 9).
A competitive assay for HSA utilizes labeled and
unlabeled antigens which are allowed to simultaneously
compete for the binding sites on the antibody. The
simultaneous exposure of the labeled and unlabeled HSA

20   to anti-HSA resulted in a constant anisotropy at all
concentrations. This may reflect a higher affinity of
anti-HSA for unlabeled HSA or the formation of
aggregates around the labeled antigen. However,
preincubation of the unlabeled HSA with anti-HSA for 30

25   minutes, followed by the addition of the Re-labeled
antigen, resulted in measurable changes in anisotropy.
In this sequential assay, the anisotropy was found to
decrease with increasing amounts of unlabeled HSA
(Figure 24). The concentrations of Re-labeled HSA and

30   anti-HSA were 2.5 μM and 4.5 μM, respectively. At high
concentrations of unlabeled HSA, the anisotropy could
not be reversed to the value for unbound Re-HSA
(r=0.017, p=0.023), which should be observed on total

38

replacement of Re-HSA with unlabeled HSA. This effect
could be explained by non-specific binding of Re-HSA to
other proteins present in the solution. However, the
polarization of Re-HSA was not influenced by the

5   presence of non-specific proteins in the IgG ascites
fluid (Figure 9). Another reason for this behavior may
be a result of a higher binding affinity for Re-HSA
than for free HSA or possibly irreversible interactions
between the Ab and Ag.

10   Example 3:
Anisotropy Probe for Protein Hydrodynamics
        Human serum albumin (HSA), bovine immunoglobulin G
(IgG), were obtained from Sigma Chemical Co. and were
used without further purification. 2,9-dimethyl-4,7-

15   diphenyl-1,10- phenanthroline (bcp), isonicotinic acid
(4-COOHPy), $AgClO_4$, NH_4PF_6, and $Re(CO)_5Cl$ were from
Aldrich Chemical Co. and used as received. The other
solvents used were of HPLC or spectroscopic reagent
grade.

20   5 mg of N,N'-dicyclohexylcarbodiimide (DCC) and 3
mg of N-hydroxy-succinimide (NHS) were dissolved in
0.15 ml of DMF with stirring, 10 mg of the Re-complex
in 0.15 ml of DMF was then added, and the mixture was
stirred for a few hours. The formed precipitate was

25   removed by filtration through a syringe filter, and the
filtrate containing the active Re-complex was used for
labeling the substrates.
        The proteins HSA and IgG (10 mg of protein) were
labeled by adding a 15-fold molar excess of the

30   activated Re-complex in 50 µl of DMF to 1 ml of stirred
protein solution (0.2 M carbonate buffer, pH 8.5),
followed by a 5 h incubation. The conjugates were
purified by gel filtration chromatography on Sephadex

39

G-25 or G-50, using 0.1 M Na_2HPO_4 - 0.1 M NaH_2PO_4 (0.1 M PBS) buffer, pH 7.0, as eluent. The dye:protein ratios of Re-HSA and Re-IgG conjugates were determined to be 2:1 and 3:1, respectively. The concentration of protein

5   was determined by the Coomassie Plus Protein Assay. The concentration of Re (I) complex was determined by its absorbance at 400 nm, assuming the extinction coefficient ($\epsilon_{400\ nm}=5040$ M^{-1} cm^{-1}) was the same as that of the free dye.

10   Fluorescence intensity and anisotropy decays were measured by time-correlated single photon counting (TCSPC). (Birch, D.J.S., and Imhof, R.E., In *Topics in Fluorescence Spectroscopy, Vol. 1: Techniques*, Lakowicz, J.R., Ed., Plenum, New York, (1991) pp. 1-

15   45). The light source was the output of a Pridine 1 dye laser, cavity dumped at 0.19 MHz and frequency doubled to 380 nm. For TCSPC measurements the emission was isolated using a long pass filter transmitting above 520 nm. The detector was a Hamamatau R2809 red-

20   sensitive microchannel plate PMT.

The time-domain intensity data were fitted by the usual procedures of nonlinear least squares and were fitted to single and multi-exponential decay laws. The intensity decays were described by Equation 9. The

25   fitting was carried out by using software from IBH Software (Edinburgh, Scotland).

The time-resolved anisotropy decays were obtained by measuring the time dependent decays of the vertically ($I(t)$) and horizontally ($I(t)$) polarized

30   components of the emission

$$r(t) = \frac{I_\parallel(t) - I_\perp(t)}{I_\parallel(t) + 2I_\perp(t)} \qquad (12)$$

40

These data were fitted to a single and double correlation time model, using the IBH software,

$$r(t) = \sum_i r_{0i} e^{-t/\theta_i}$$

(13)

where r_{0i} are the amplitudes and θ_i are the rotational correlation times.

The excitation anisotropy spectra were collected as usual, with the anisotropy defined by

$$r(\lambda) = \frac{I_{\parallel}(\lambda) - I_{\perp}(\lambda)}{I_{\parallel}(\lambda) + 2 I_{\perp}(\lambda)}$$

(14)

Steady-state fluorescence data were obtained using a spectrofluorometer from SLM Instruments, with magic-angle polarizer conditions and a Hamamatsu R-928 detector. The emission spectra are uncorrected for the wavelength dependence of the detection system.

The molecular structure of $[Re(bcp)(CO)_3(4-COOHPy)]^+$ is shown in Figure 1. The absorption and excitation spectra of the Re-complex in CH_3OH are shown in Figure 25. The absorption spectra of the ligands in CH_3OH are also shown for comparison. The spectra are normalized to unity to facilitate comparison. The absorption spectral maxima of the low-energy absorption band around 340 ~ 450 nm and the more intense higher energy absorption at 298 nm are the characteristic metal-to-ligand charge transfer (MLCT) and $\pi-\pi^*$ absorption, respectively. The emission originates from MLCT states, with two maximal excitation bands at ~345 nm and ~390 nm, respectively. It is important to note that a complex with absorption near 380 nm can be excited with the UV output of a light emitting diode.

41

The emission spectra of Re-complex in $CHCl_3$, CH_3OH and
Re-HSA and Re-IgG conjugates are shown in Figure 26.
The large Stokes' shift of the Re-complex and its
protein conjugates (~100 nm) makes it a good candidate
5   for energy transfer studies and other biopysical
studies as there is no possibility for self quenching.
This Re-complex displays high quantum yields (>0.5) in
fluid solutions at room temperature. The influence of
oxygen is modest when it is bound to macromolecules.

10   To be useful as an anisotropy probe for study of
macromolecular dynamics, the Re-complex needs to
display polarized emission. We studied the polarized
emission in the absence of rotational diffusion. The
excitation anisotropy spectra of $[Re(bcp)(CO)_3(4-$
15   COOHPy)]$^+$ and its protein conjugates, Re-HSA and Re-IgG,
are shown in Figure 27. In the absence of rotational
motion, this complex shows maximal anisotropies near
0.3 and these high anisotropies are broadly available
from 390 nm to 450 nm. The steady-state anisotropy of
20    $[Re(bcp)(CO)_3(4-COOHPy)]^+$ and its conjugates were
measured as a function of temperatures and/or
viscosities (Figure 28). The solvent used for this
study was 60% glycerol/40% buffer (v/v), which formed a
highly viscous solution at -60 °C. The results show that
25   the anisotropy values are nearly the same for the free
dye and the Re-protein conjugates at -60 °C. The steady-
state anisotropy of the free $[Re(bcp)(CO)_3(4-COOHPy)]^+$
decreases rapidly as the temperatures are changed from
low temperature, -60 °C towards high temperature, 20 °C,
30   whereas the anisotropies of Re-HSA and Re-IgG decrease
more slowly with temperature, and remain adequate for
measurement at room temperature. These results
demonstrate that the anisotropies are sensitive to
rotational motion, and the anisotropy of the Re-protein

42

conjugates is lost by fast motions of the probe in
addition to rotational motion of the proteins.
Importantly, the anisotropies of the labeled protein
are always larger than that of free dye, indicating

5   that protein hydrodynamics contributes to the
anisotropy.

To further demonstrate that the anisotropy depends
on rotational diffusion we examined the time-dependent
anisotropy of free [Re(bcp)(CO)$_3$(4-COOHPy)]$^+$ in 100%

10   glycerol and 60% glycerol/40% buffer (v/v) at -60 °C and
20 °C. At 20 °C, the anisotropy decays rapidly with a
correlation time near 4 ns in 60% glycerol/40% buffer
(v/v), whereas the anisotropy decays more slowly with a
correlation time of 118 ns in 100% glycerol. At -60 °C,

15   the anisotropy decays much more slowly with a
correlation time 82 μs in 100% glycerol (Figure 29).

Time-resolved anisotropy decays of Re-protein
conjugates are shown in Figure 30. Analysis of these
anisotropy decays are summarized in Table 3.

43

Table 3. Time-resolved Intensity Decay (τ), Rotational Correlation Times (θ) of free $[Re(bcp)(CO)_3(4\text{-COOHPy})]^+$ and its protein conjugates.

Sample	τ_i (ns)	f_i*	χ_R^2	θ_i (ns)	r_{io}	χ_R^2
ReCOOH in 60% glycerol	1478	1	1.2	4	0.0713	0.97
RE-HSA in 60% glycerol	7	0.0024		12	0.168	
	79	0.021		457	0.0789	1.0
	1402	0.98	1.1			
Re-HSA in 30% glycerol	10	0.0089		12	0.157	
	952	0.93		282	0.104	1.0
	1068	0.063	1.1			
Re-HSA in buffer	18	0.02		16	0.143	
	781	0.84		164	0.0788	1.2
	143	0.14	1.2			
Re-IgG in 60% glycerol	14	0.0014		6	0.0614	
	1986	0.97		379	0.0384	2.0
	153	0.025	1.0			
Re-IgG in buffer	21	0.0088		10	0.0800	
	606	0.86		271	0.0595	1.2
	134	0.13	1.1			

$$* \quad f_i = \frac{\alpha_i \tau_i}{\sum_i \alpha_i \tau_i}$$

Free $[Re(bcp)(CO)_3(4\text{-COOHPy})]^+$ anisotropy decay are fitted to single exponential anisotropy decay model, whereas the anisotropy decays of Re-labeled protein are fitted to a double exponential decay model, reflecting

44

a fast motion of the probe and a slower protein
rotational diffusion. In addition, the anisotropy decay
of labeled IgG appears to be somewhat more complex than
labeled HSA, suggesting that independent domain motions

5   of IgG contribute to the anisotropy decay. The results
demonstrate that the anisotropy decays are dependent on
protein rotational diffusion and inter-domain dynamics.
The anisotropy decays are slowed by adding glycerol as
a result of the slower protein rotational diffusion.

10   Example 4:
       Red Fluorescent Dyes for Biophysics and for Sensors
           All chemicals and solvents were purchased from
       Aldrich Chemical Co. and used without further
       purification. The ligand tppz was purchased from GF

15   Chemicals and recrystallized before use, and ligands
       ttpy (Spahni, W. And Galzaferri, G. *Helv. Chim.Acta.*,
       1984, 67, 450; Constable, E.C. and Thomson, A.M., *J.
       Chem. Soc., Dalton Trans.* (1994) 2947) and mcbpy
       (Strouse, G.F., Schoonover, J.R., Duesing, R., Boyed,

20   S., Jones, W.E. Jr., Meyer, T.J., *Inorg. Chem.*, 1995,
       34, 473) were synthesized using reported procedures.
           All absorbence spectra were recorded on a Hewlett
       Packard diode array (HP 8453) spectrophotometer. All
       emission spectra were recorded on a SLM AB2

25   spectrophotometer. The excitation anisotropy spectra
       were measured at -55 °C in 9:1, glycerol:methanol by
       weight, using a SLM 800 spectrophotometer. Excitation
       anisotropy spectra were collected as usual, with the
       anisotropy defined by Equation 5, where $I_{\parallel}$ and $I_{\perp}$ are

30   the intensities measured with vertically polarized
       excitation and the emission polarization parallel ($\parallel$)
       or perpendicular ($\perp$) to the excitation. The values of

45

the polarized intensities were corrected for the
transmission efficiency for the polarized components by
the detection optics. The reported emission spectra are
corrected for variation in the detector efficiency with
observation wavelength.

Fluorescence intensity decays were measured with
frequency-domain instrumentation (Laczko, G. Grycznski,
I., Wiczk, W., Malak, H. and Lakowicz, J.R., *Rev. Sci.
Instrum.* 1990, 61, 2331). The excitation wavelength was
488 nm using an air cool argon laser supplied by
Omnichrome Inc. The frequency-domain data were used to
determine the intensity decay law using
multiexponential model

$$I(t) = \sum_{i=1}^{n} \alpha_i e^{-t/\tau 1} \tag{15}$$

where α_i are the preexponential factors, τ_i are decay
times, and n is the number of exponential components.
The mean decay time is given by

$$\overline{\tau} = \alpha_i \tau_i^2 / \Sigma \alpha_j \tau_j \tag{16}$$

Synthesis of Complexes

All of these complexes were synthesized as PF$_6$
salts by following two different methods which depend
on the ligand used. Method A describes the synthesis of
complexes using tridentate ligands (L-L-L) generally
ttpy, tpy, tppz and triphos. Method B describes the
synthesis of complexes using bidentate ligands (L-L)
which are consist of mcbpy, phen and aphen ligands.
Both methods are modifications of reported methods

46

(Kober, E.M., Marshall, J.L., Dressick, W.J., Sullivan,
B.H., Casper, J.V. and Mayer, T.J. *Inorg. Chem.*, (1984)
24, 2755; Brewer, R.G., Jensen, G.E. and Brewer, K.J.
Inorg. Chem., (1994) 33, 124; Kober, E.M., Marshall,

5   J.L., Dressick, W.J., Sullivan, B.H., Casper, J.V. and
Meyer, T.J. *J. Am. Chem. Soc.*, (1980) 102, 7385; Arana,
C.R. and Abruna, H.O. *Inorg. Chem.* (1993) 32, 194;
Sauvage, J.P., Collin, J.H., Chambron, J.C., Guillerez,
S.Coudret, C., Balzani V., Bariegelleti, F., Cola,

10   L.D., and Flamigni, L., *Chem. Rev.* (1994) 94, 993).

*Synthesis of [Os(L-L-L)₃]²⁺, with Tridentate Ligands
(Method A)*

In this typical synthesis, one equivalent of $OsCl_3$

15   and one equivalent of tridentate ligands, L-L-L, (where
L-L-L is either ttpy, tppz or triphos) was heated at
reflux in 100 ml of ethanol, and a black precipitate
of $Os(L-L-L)Cl_3$ forms after three hours of heating. This
precipitate was filtered after cooling and washed with

20   water and ethanol. This is the starting material for
the desired compounds, $[Os(L-L-L)_3]^{2+}$. Equal molar
ratios of $Os(L-L-L)Cl_3$ and the appropriate ligand were
further heated at reflux in 20 ml of ethylene glycol
for one hour, which produces a brown solution. After

25   cooling, about 100 ml of a saturated solution of
ammonium hexafluorophosphate in water was added. After
a few minutes, a dark brown-black precipitate formed.
This precipitate was separated out by vacuum filtration
and dried. All these compounds were recrystallized

30   after dissolving them in acetonitrile and crystallizing
them by using an excess amount of ether. They were
chromatographed on neutral alumina using a 5:2
toluene:acetonitrile mixture.

47

Synthesis of [Os(L-L)₃]²⁺, with Bidentate Ligands (Method B)

The starting material, $Os(L-L)_2Cl_2$, for all these compounds was synthesized by mixing one equivalent of

5   $(NH_4)_2OsCl_6$ and two equivalents of bidentate ligands L-L, (where L-L are either mcbpy, phen or aphen). This reaction mixture was heated at reflux for about one hour in 50 ml of ethylene glycol. A dark brown precipitate was obtained which was filtered and washed

10 with water and ethanol. For making $[Os(L-L)_3]^{2+}$ complexes, equal molar ratios of $Os(L-L)_2Cl_2$ and the appropriate ligand were further heated at reflux in 20 ml of ethylene glycol for about six hours, which produced a greenish brown solution. After cooling this

15 reaction mixture, about 100 ml of a saturated solution of ammonium hexafluorophosphate in water was added, and a dark green precipitate separated out. The precipitate was filtered by vacuum filtration and dried. These dried compounds were recrystallized by

20 dissolving them in acetonitrile and crystallizing them out by adding a large amount of ether. It was chromatographed on neutral alumina using a 2:1 toluene:acetonitrile mixture.

Electronic Absorption Spectroscopy

25 The electronic spectra of these osmium complexes in acetonitrile are shown in Figure 11 and summarized in Table 4.

48

Table 4.   Spectral properties of the red osmium probes

Probes[a]	λ_{max}^{abs} (nm)[b]	λ_{max}^{em} (nm)[b]	τ(ns)[c]	ϕ^c	r_o^d
[Os(ttpy)₂]²⁻	500	735	220	0.02	0.15
[Os(3,2,1)]²⁻	550	640	130	0.015	--
[Os(tpy)(triphos)]²⁻	470	710	230	--	0.35
[Os(phen)₂(aphen)]²⁺	485	700	195	0.02	0.02
[Os(tppz)₂]²⁻	480	740	175	0.016	0.18

[a] All are PF₆ salts; [b] measured in acetonitrile;
[c] measured in deoxygenated acetonitrile; [d] measured in
9:1 glycerol:methanol mixture at -55°C.

The ultraviolet region of the tridentate ligands are
similar to each other and are dominated by the π→π*
transitions from the ligand. The visible region of the
electronic spectra of tridentate complexes contains
intense bands centered between 450-500 nm. These
transitions represent the lowest lying ¹MLCT, which is
Os(dπ)→L-L-L(π*) in nature for all these complexes. Due
to the high degree of spin-orbit coupling in osmium,
transitions that are formally spin forbidden exhibit
enhanced intensity. (650 nm). These MLCT transitions
appear as tails on the low energy end of the more
intense ¹MLCT transition.

49

Emission Spectroscopy, Quantum Yields and Excited State Lifetimes

The emission maxima, quantum yields, and lifetimes are outlined in Table 4. All these complexes emit at
5   700-750 nm at room temperature, Figure 12, when they are excited at 480 to 550 nm. Similar trends are seen in the emission and absorption energies of all these complexes. All of these complexes have excited-state lifetimes around 200 ns. The lifetime of the
10    $[Os(tppz)_2]^{2+}$ complex was found to be 175 ns. The quantum yields of all these complexes are around 2 percent which is typical for all these red emitting osmium(II) complexes (Kober, E.M., Marshall, J.L., Dressick, W.J., Sullivan, B.H., Casper, J.V. and Mayer,
15   T.J. *Inorg. Chem.*, (1984) 24, 2755; Sauvage, J.P., Collin, J.H., Chambron, J.C., Guillerez, S. Coudret, C., Balzani, V., Barigelleti, F., Cola, L.D., and Flamigni, L., *Chem. Rev.* (1994) 94, 993).

Fundamental Anisotropy (r_0).

20   Anisotropy of these complexes are measured in 9:1 (glycerol:methanol by weight) at -55 °C and summarized in Table 4, and shown in Figure 13. The trend of the anisotropy depends on the structure of the molecules. More asymmetric molecules show higher anisotropies. The
25   complex $[Os(tpy)(triphos)]^{2+}$ is the most asymmetric molecule, and therefore shows a high anisotropy value (0.35).

Since many modifications, variations, and changes in detail may be made to the described embodiments, it
30   is intended that all matter in the foregoing description and shown in the accompanying drawings be

50

SUBSTITUTE SHEET (RULE 26)

interpreted as illustrative and not in a limiting
sense.

51

CLAIMS

1.   A method of conducting an assay of a sample containing an analyte of interest, comprising the steps of:

    5
        forming a mixture so as to bring a metal-ligand complex into interactive proximity with said sample containing said analyte of interest;

        irradiating said mixture with electromagnetic light energy so as to cause emission of light indicative of said analyte of interest; and

    10
        measuring the emitted light and utilizing the measurement of the emitted light so as to measure the analyte of interest.

2.   A method as defined by claim 1, wherein said assay is used to characterize a high molecular weight antigen.

    15

3.   A method as defined by claim 2, wherein said analyte of interest is human serum albumin.

4.   A method as defined by claim 1, wherein said assay is used to characterize protein hydrodynamics.

    20

5.   A method as defined by claim 4, wherein said analyte of interest is human serum albumin and bovine immunoglobin G.

6.   A method as defined by claim 1,

    25
        wherein said assay is used to characterize a sample lipid; and

        wherein said metal-ligand complex is coupled to a lipid so as to form a lipid-probe complex.

52

7.   A method as defined by claim 1, wherein said assay is used for oxygen sensing.

8.   A method as defined by claim 1,
      wherein said assay is used to quantify said
5   analyte of interest;
      wherein prior to said forming step, a first
binding partner and a second binding partner are
added to said sample, wherein said first binding
partner competes with the analyte for binding to
10   said second binding partner, wherein one of said
first and second binding partner is labeled with a
metal-ligand complex and the other is labeled with
a photoluminescent energy transfer acceptor,
wherein the metal-ligand complex and
15   photoluminescent energy transfer acceptor are
chosen such that when the first binding partner
binds to the second binding partner, the metal-
ligand complex and the photoluminescent energy
transfer acceptor are brought into interactive
20   proximity, producing a detectable change in
luminescence.

9.   A method as defined by claim 8,
      wherein subsequent to said measuring step,
25   binding of the first binding partner to the second
binder partner is quantified; and
      wherein said binding is quantified by a
method from the group consisting of intensity,
lifetime, and polarization, thereby quantifying
30   the analyte.

10.   A method as defined by claim 1, wherein fluorescence lifetime is measured.

53

11. A method as defined by claim 1, wherein said metal-ligand complex is coupled to said analyte of interest.

12. A method as defined by claim 1, wherein said
5   metal-ligand complex is selected from the group consisting of Ru(II), Os(II), and Re(I).

13. A method as defined by claim 12, wherein said metal-ligand complex is selected from the group consisting of mono, bis, and tri(heteroleptic)
10 complexes of Ru(II) and Os(II) and carbon monoxide diimine complexes of Re(I).

14. A method as defined by claim 1, wherein said metal-ligand complex is selected from the group consisting of $[Re(bcp)(CO)_3(4-COOHPy)]^+$,
15 $[Os(phen)_2(aphen)]^{2+}$, $[Os(tpy)(triphos)]^{2+}$, $[Os(tppz)_2]^{2+}$, and $[Os(ttpy)_2]^{2+}$.

15. A method as defined by claim 1, wherein said ligand is selected from the group consisting of ligands based on diimine, phosphine, arsine, pyridine,
20 substituted pyridines, carbon monoxide, carbonyl, and any combination thereof.

16. A method as defined by claim 15, wherein said ligand is substituted with a functional group that can be directly conjugated to macromolecules selected from
25 the group consisting of amine reactive N-hydroxysuccimide, isothiocyanate, sulfonyl chloride containing ligands, sulfhydryl reactive iodoacetadmide, and maleimide containing ligands.

54

17. A method as defined by claim 1,
     wherein said electromagnetic light energy is
linearly polarized light energy; and
     wherein polarization of the emitted light is
5   measured.

18. A method as defined by claim 17, wherein said
linearly polarized light energy has a wavelength of
about 400.

19. A method as defined by claim 17, wherein said
10   linearly polarized high energy has a wavelength from
280 to 1100 nm.

20. A metal-ligand complex of the formula
[Re(bcp)(CO)$_3$(4-COOHPy)]$^{\cdot}$.
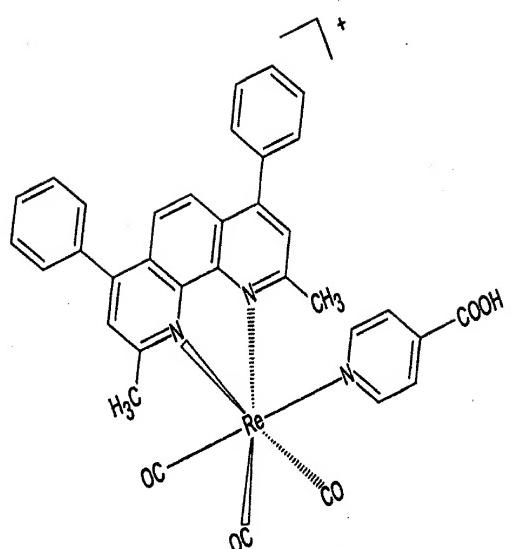
FIG. 1

FIG. 2

FIG. 3

FIG. 4

FIG. 5

FIG. 6

FIG. 7

FIG. 8

FIG. 9

[Os(phen)₂(aphen)]²⁺

FIG. 10A

[Os(tpy)(triphos)]²⁺

FIG. 10B

FIG. 11

FIG. 12

FIG. 13

$\tau = 175$ ns

$-O_2$

$\tau = 145$ ns

$+O_2$

$Os(tppz)_2^{2+}$

COUNTS

10^3

10^2

TIME/10^{-8} SEC.
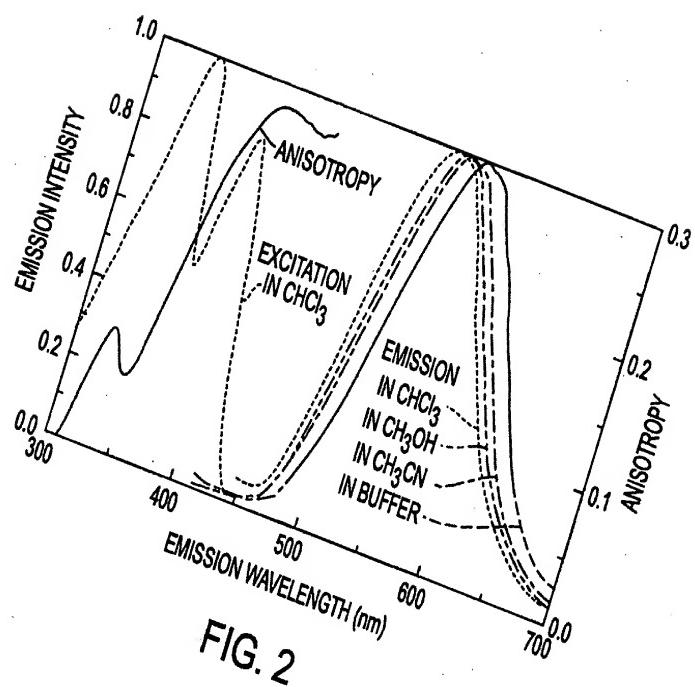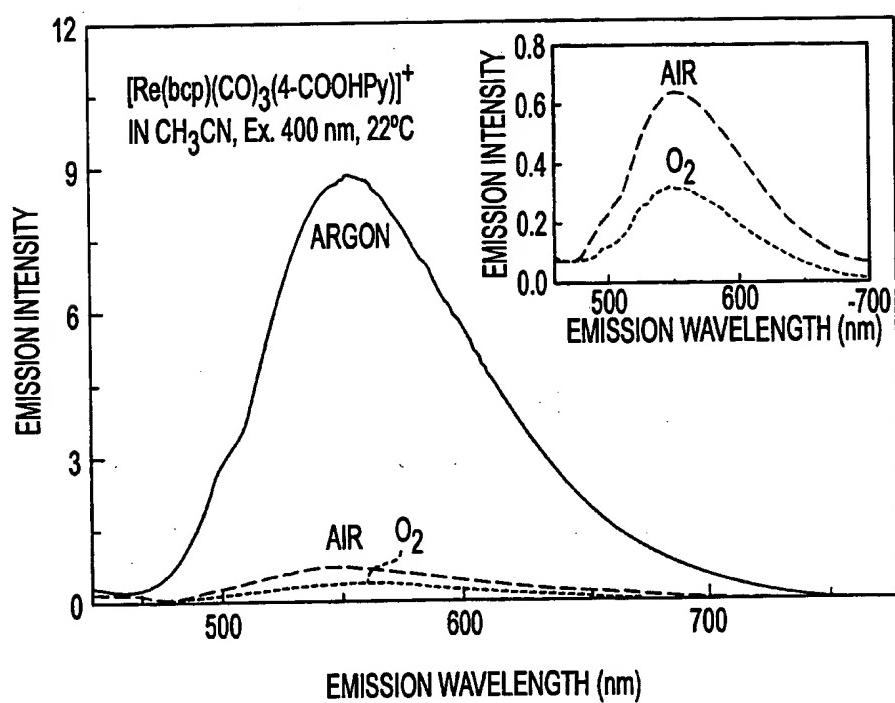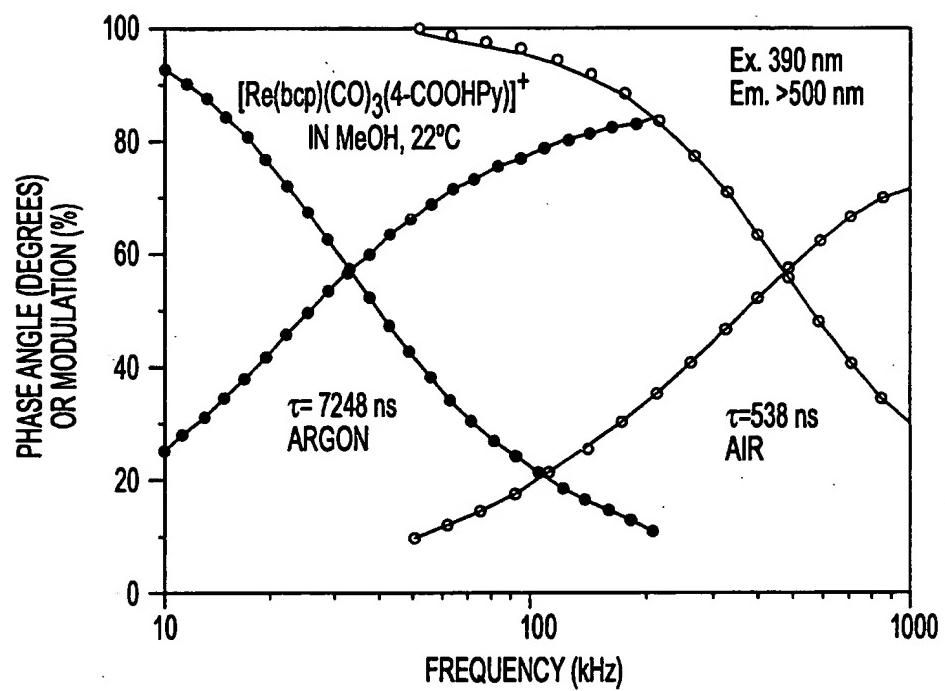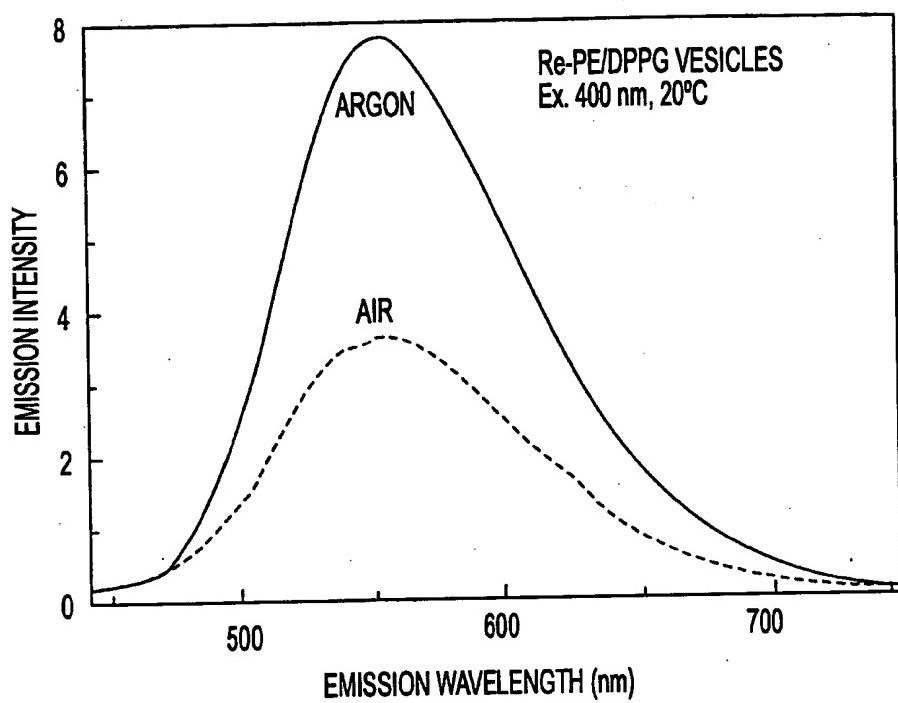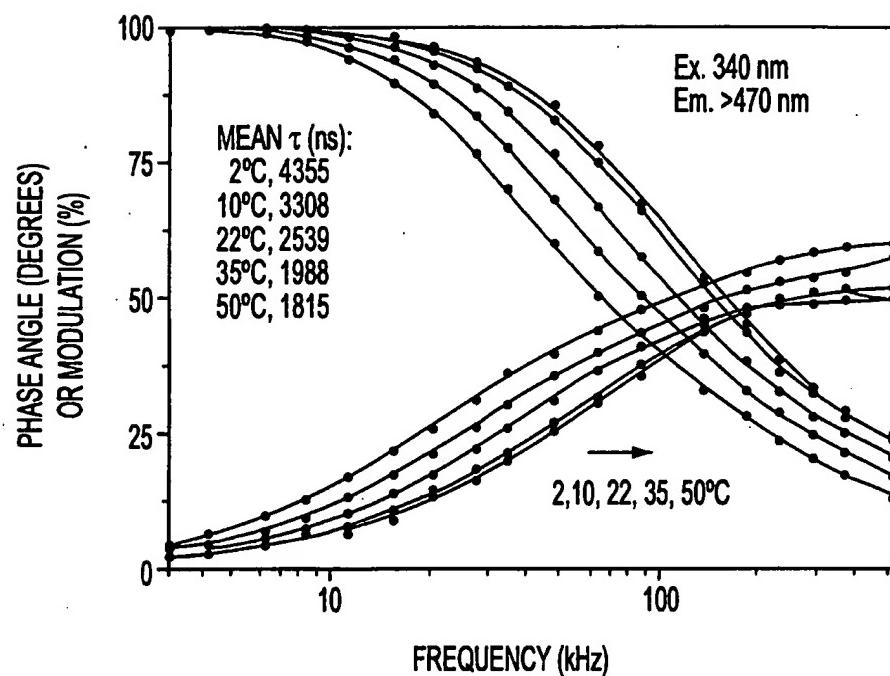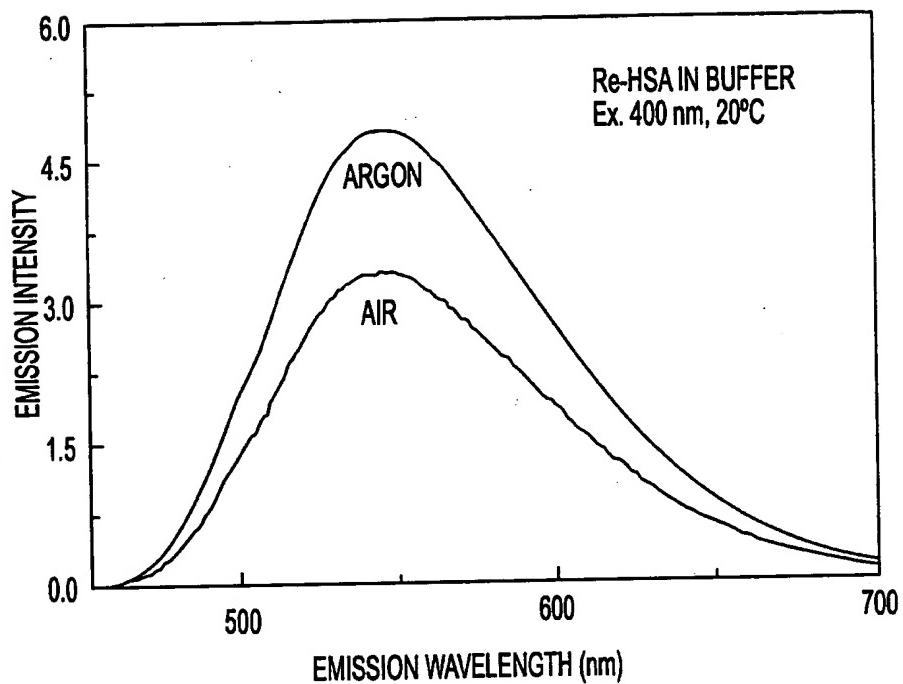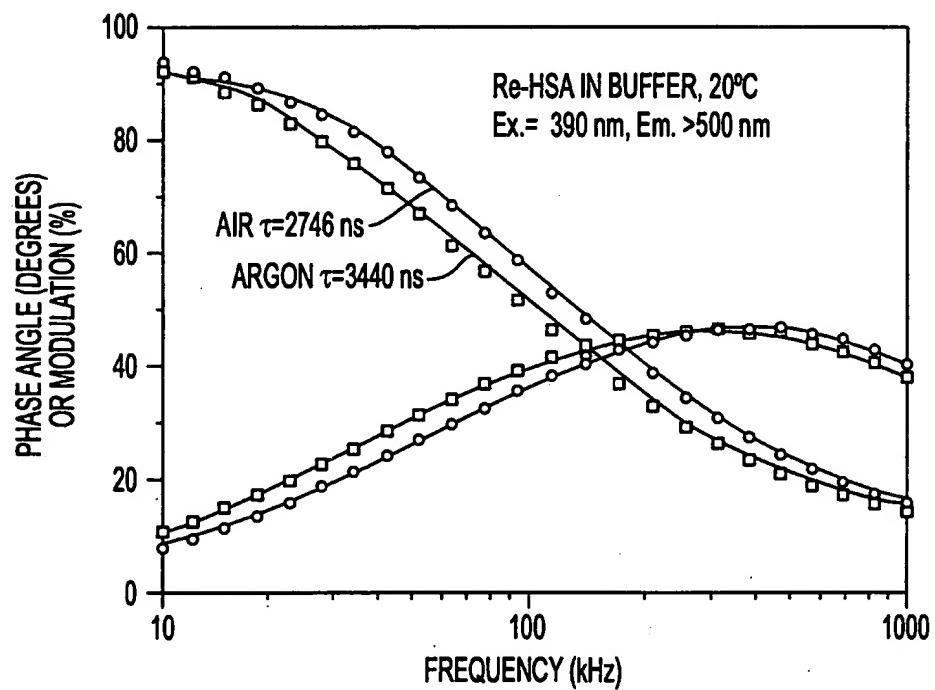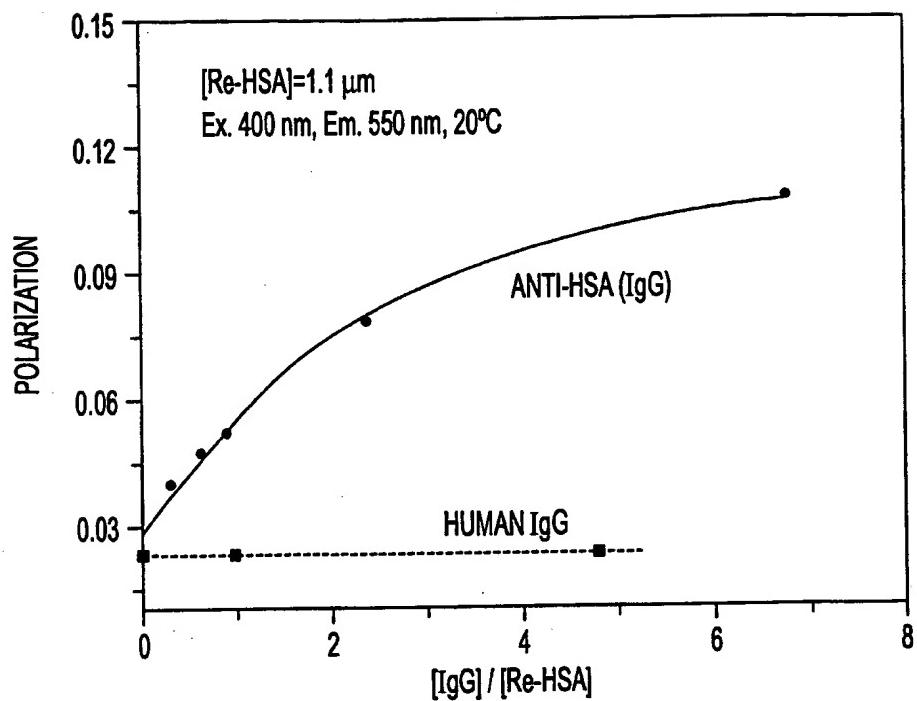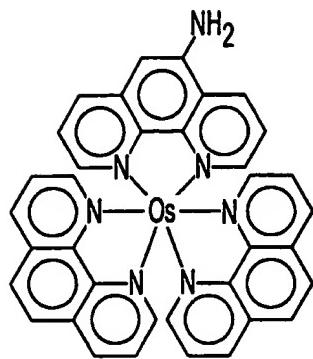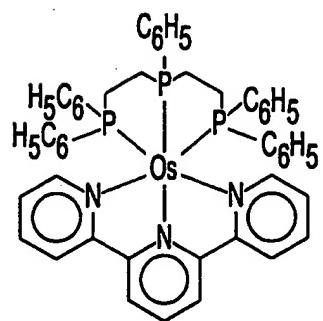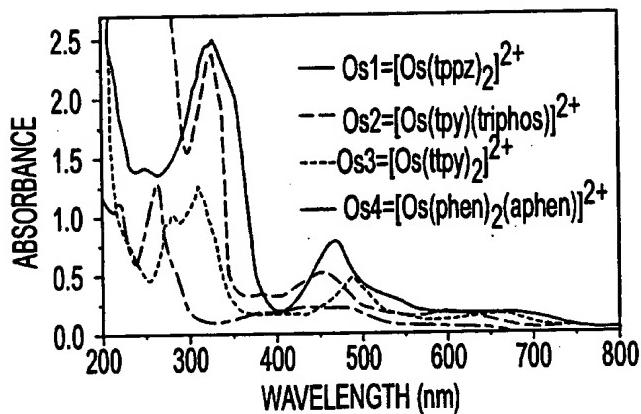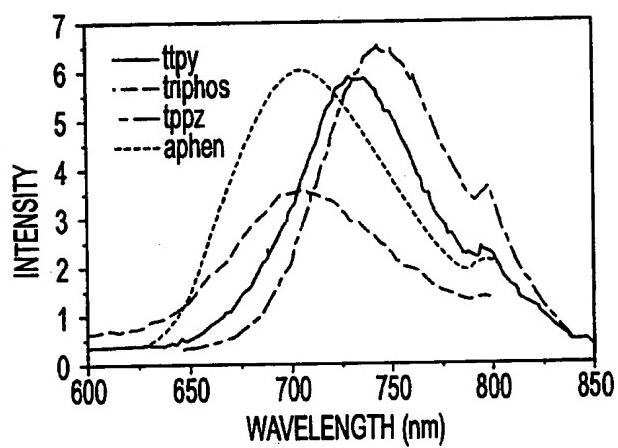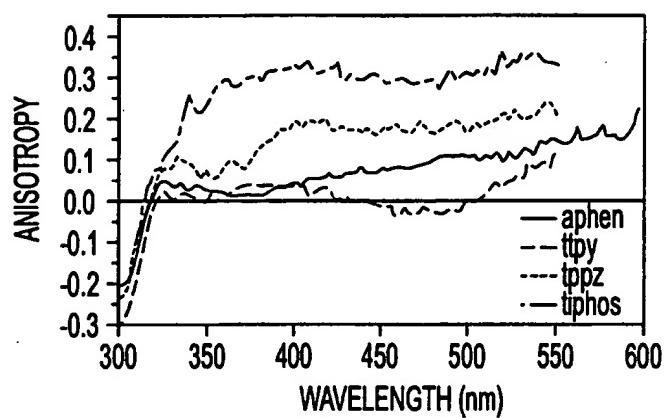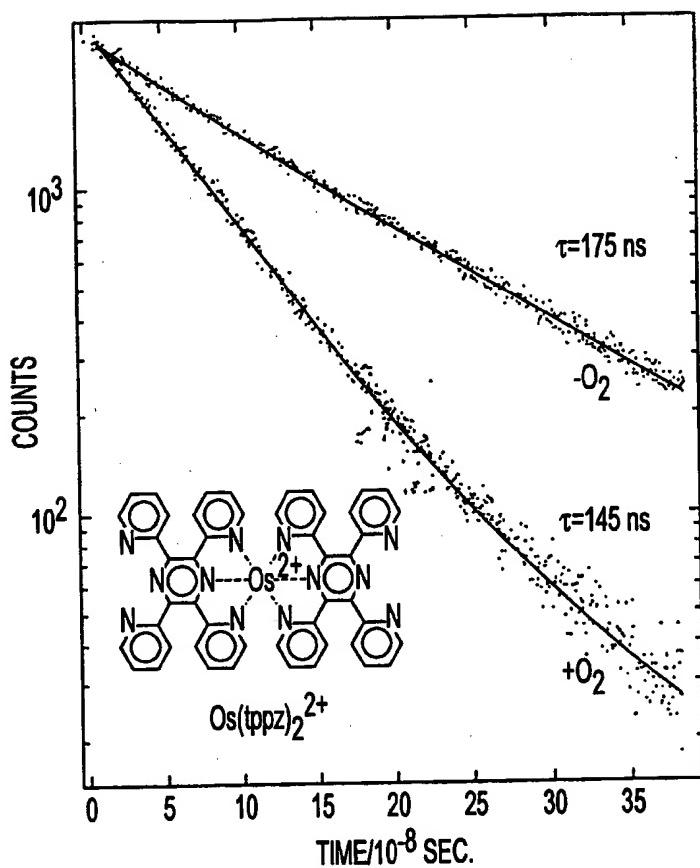
FIG. 14
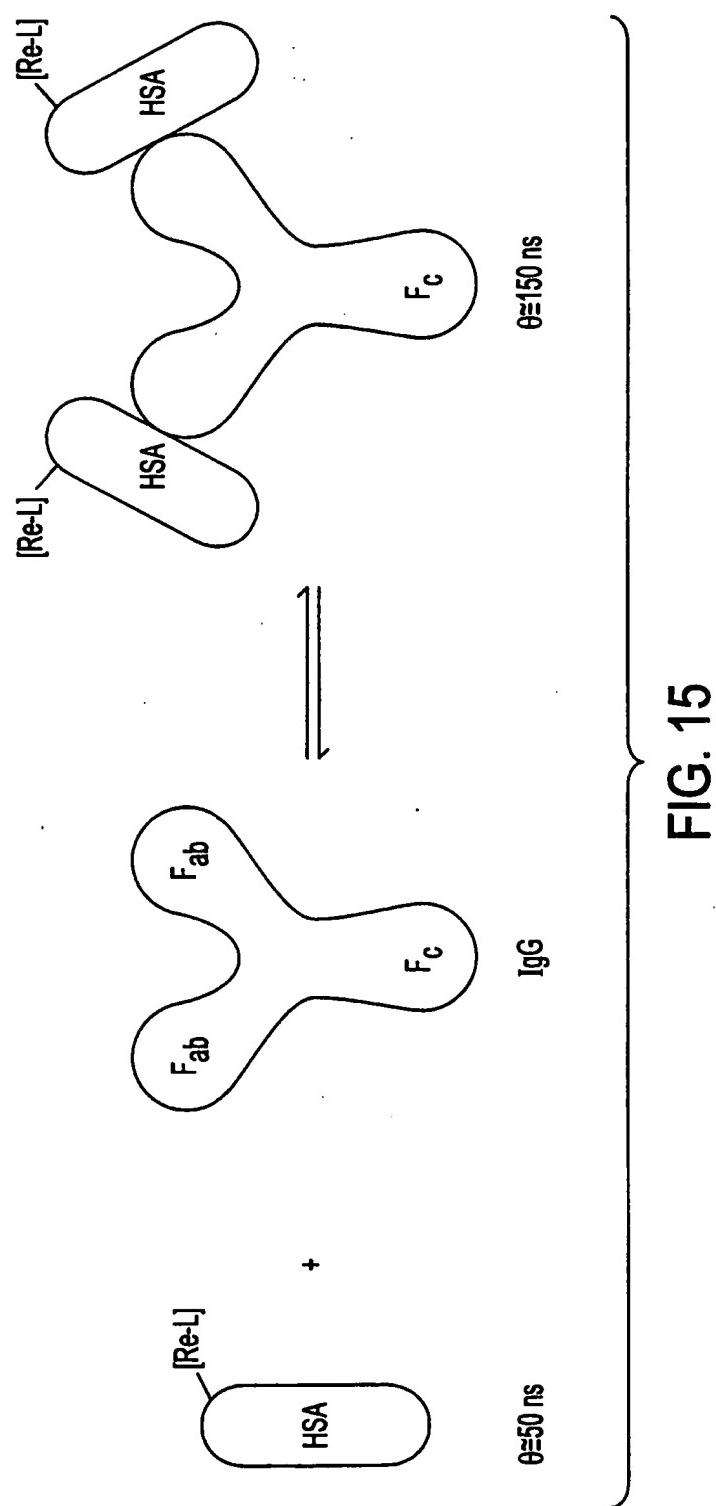
FIG. 15
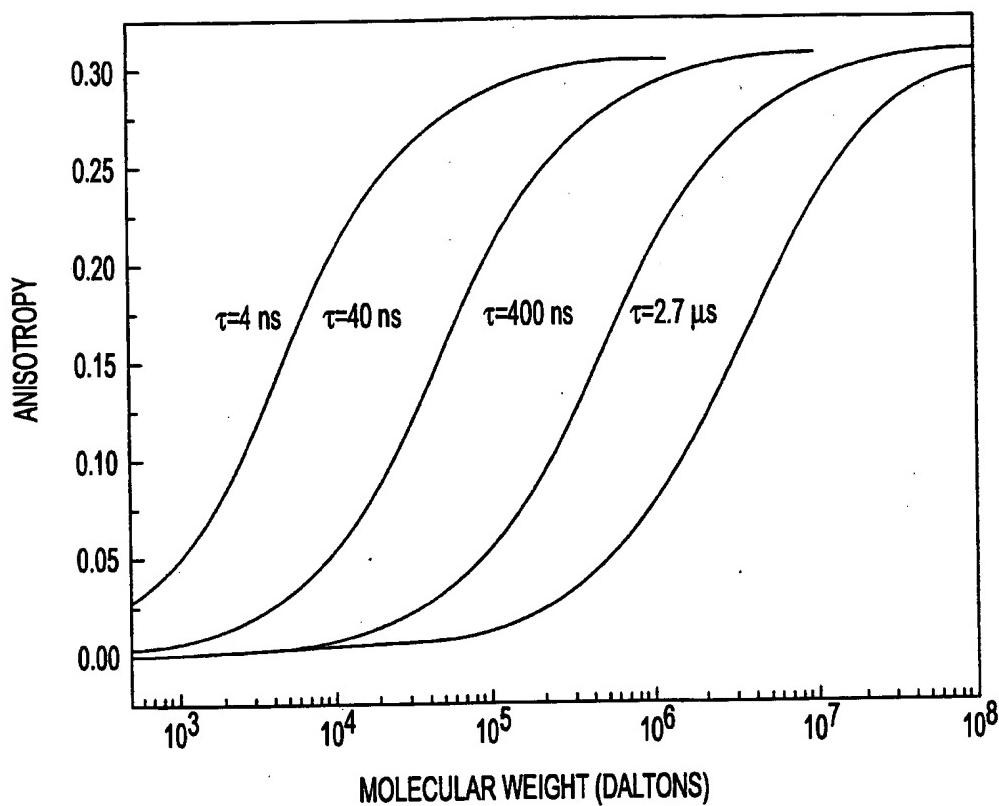
FIG. 16
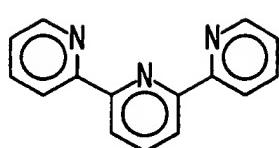
2,2':6,2"-terpyridine (tpy,3)
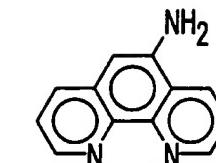
FIG. 17A

5-amino-phenanthroline (aphen)

FIG. 17B

Pyridine (py,1)

FIG. 17C

4-methyl,2,2'-bipyridine-4'-carboxylic acid (mcbpy,2)
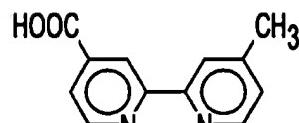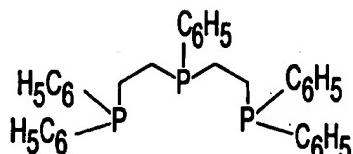
FIG. 17D

Bis(2-diphenylphosphinoethyl)phenyl phosphine (triphos)

FIG. 17E
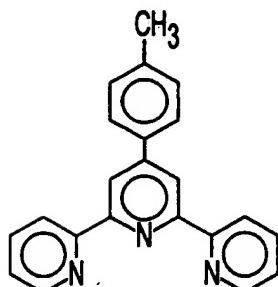
4-tolyl, 2,2':6,2"-terpyridine (ttpy)
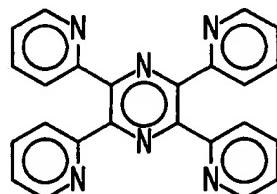
FIG. 17F

2,3,5,6-tetrakis(2-pyridyl)pyrazine(tppz)

FIG. 17G
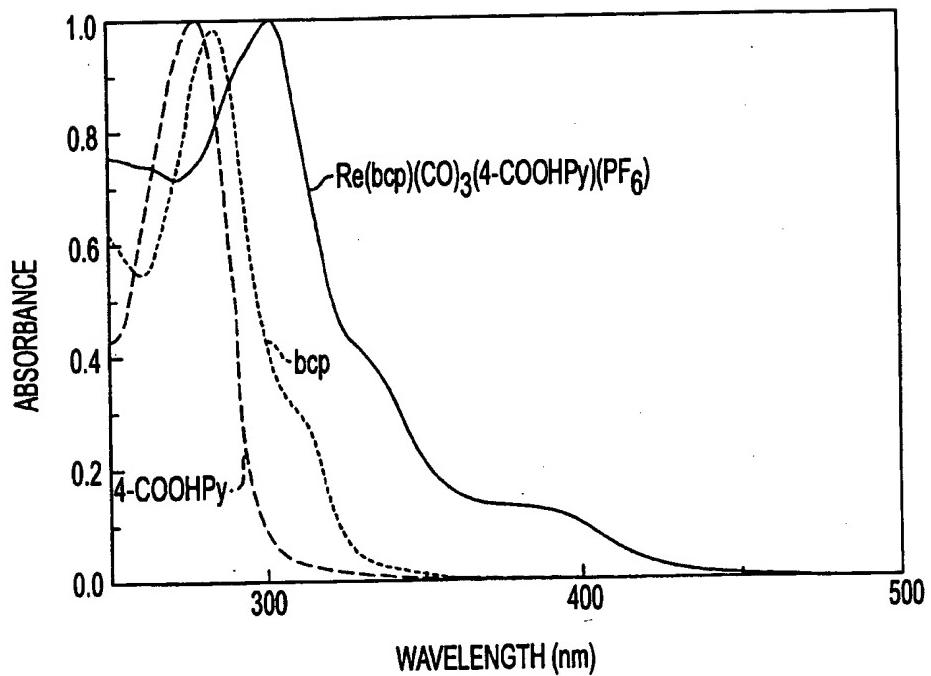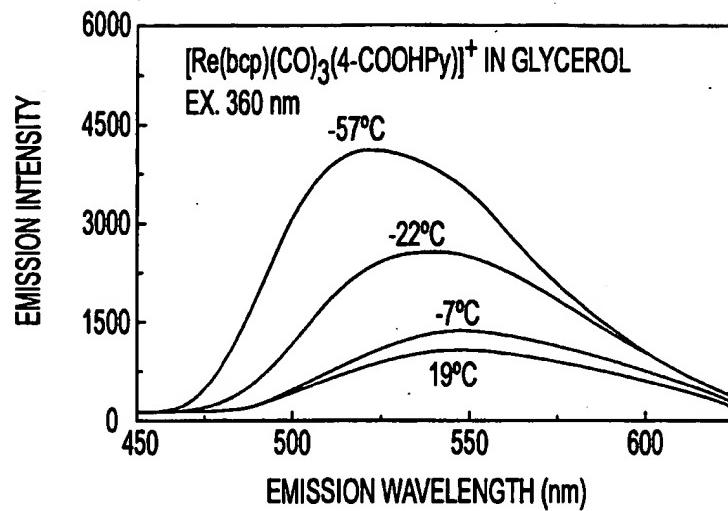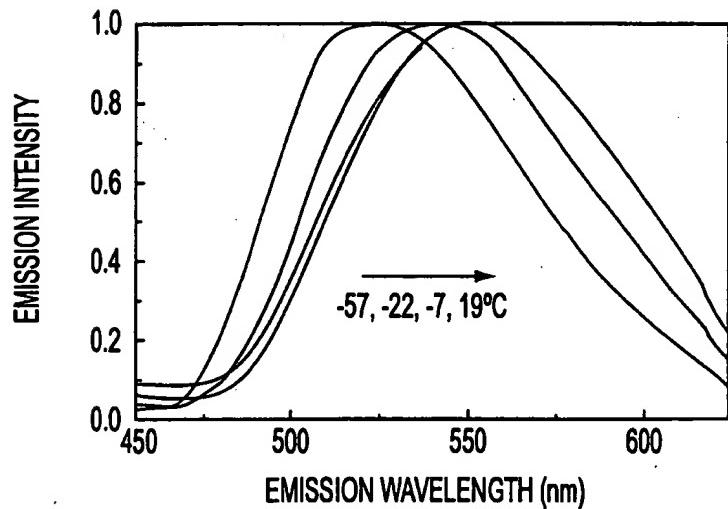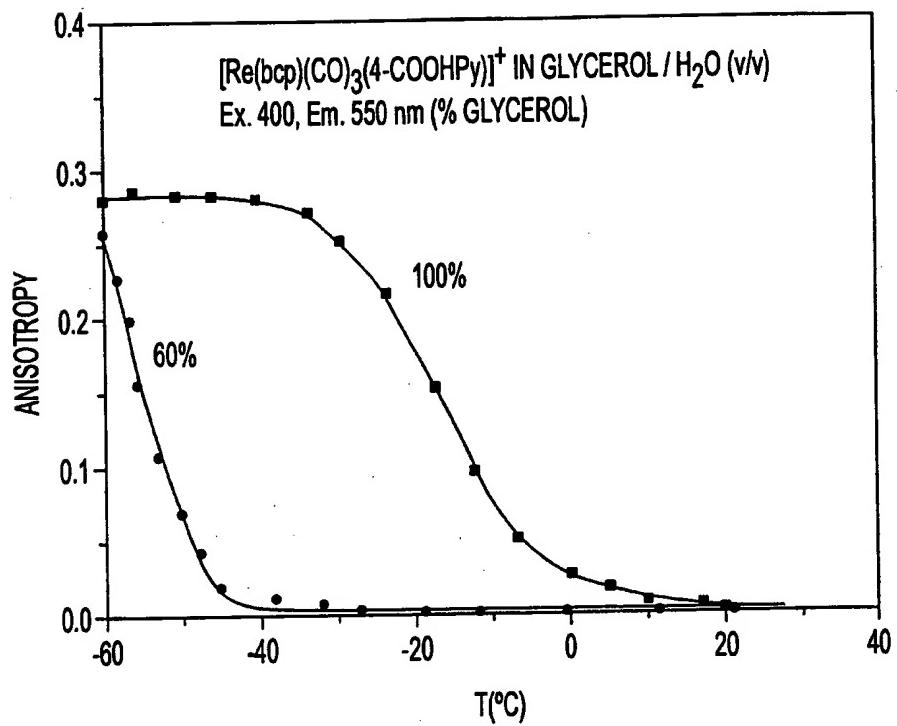
FIG. 18

[Re(bcp)(CO)$_3$(4-COOHPy)]$^+$ IN GLYCEROL
EX. 360 nm

-57°C
-22°C
-7°C
19°C

EMISSION INTENSITY

EMISSION WAVELENGTH (nm)

FIG. 19A

EMISSION INTENSITY

-57, -22, -7, 19°C

EMISSION WAVELENGTH (nm)

FIG. 19B

FIG. 20

[Re(bqp)(CO)₃(4-COOHPy)]⁺ IN CH₃CN
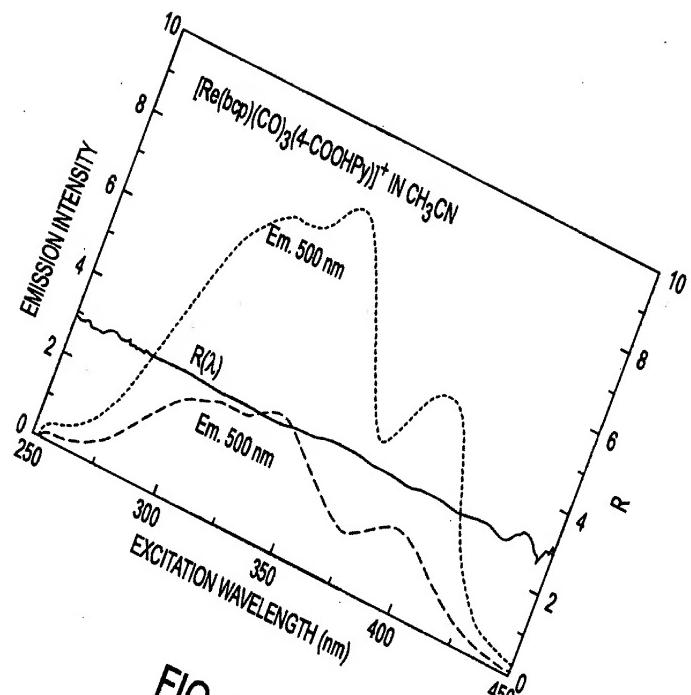
FIG. 21
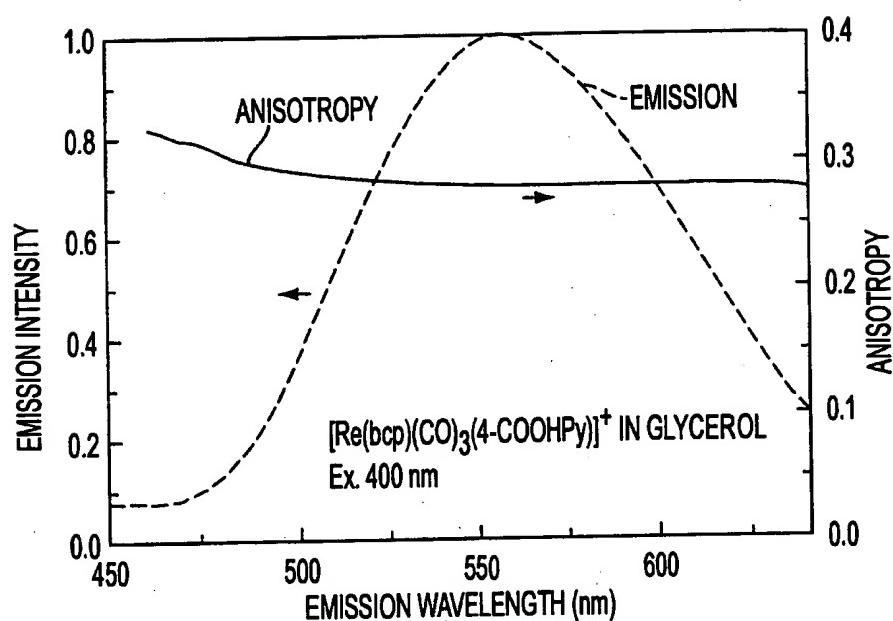
FIG. 22
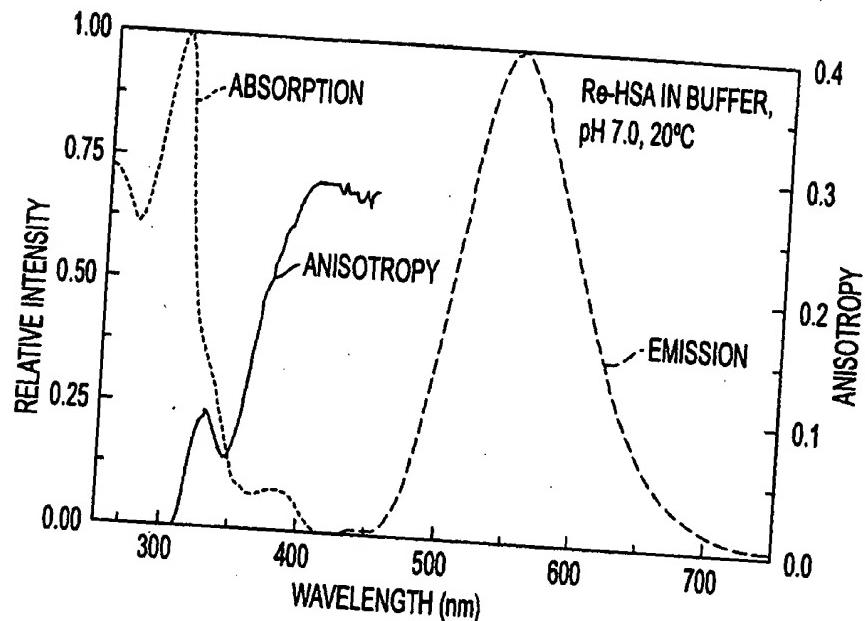
FIG. 23
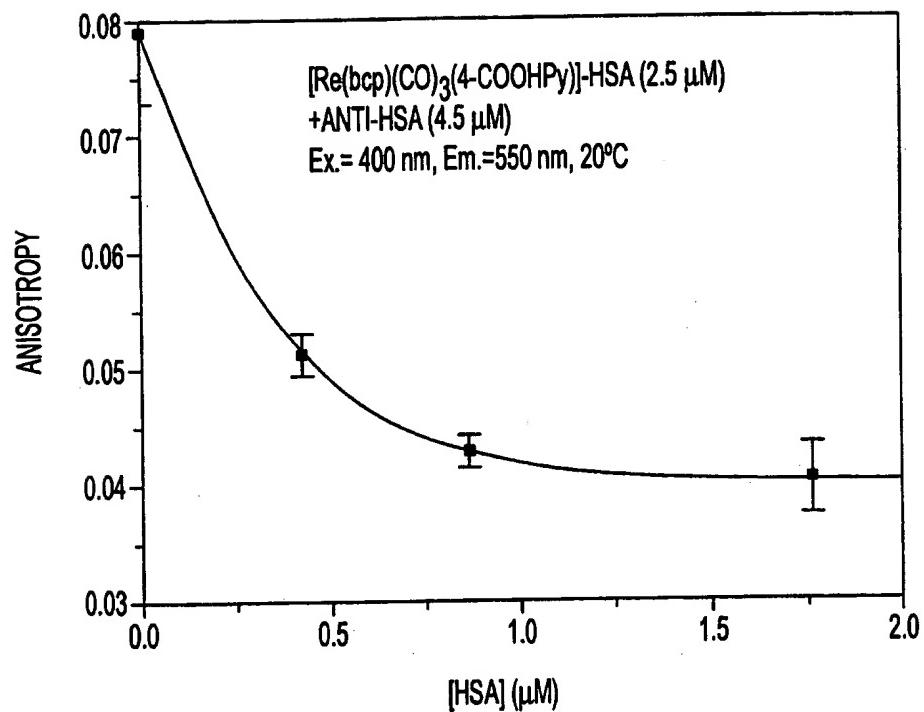
FIG. 24
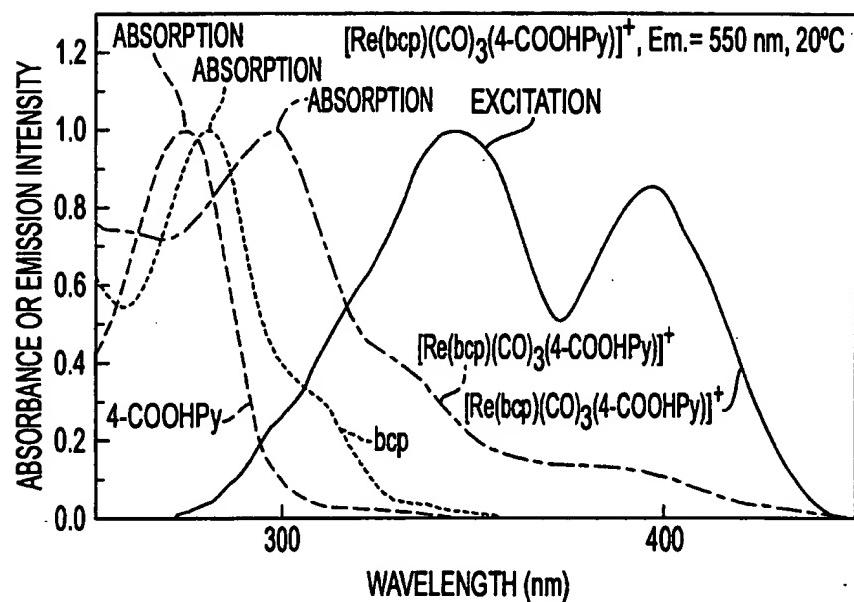
FIG. 25
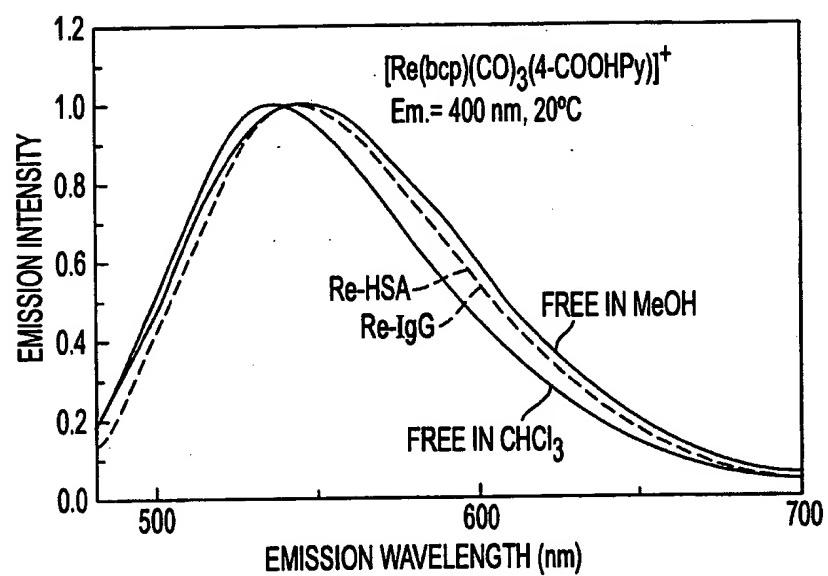
FIG. 26
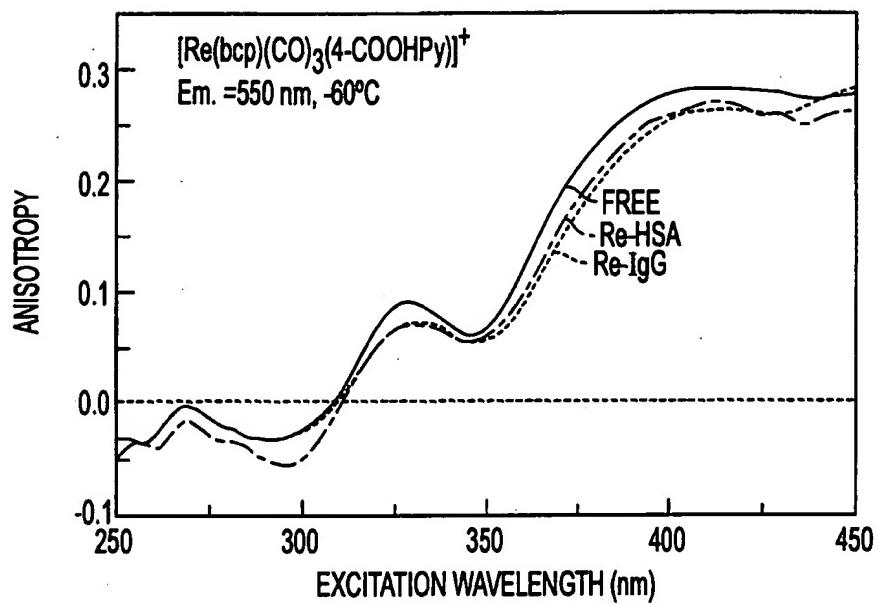
FIG. 27
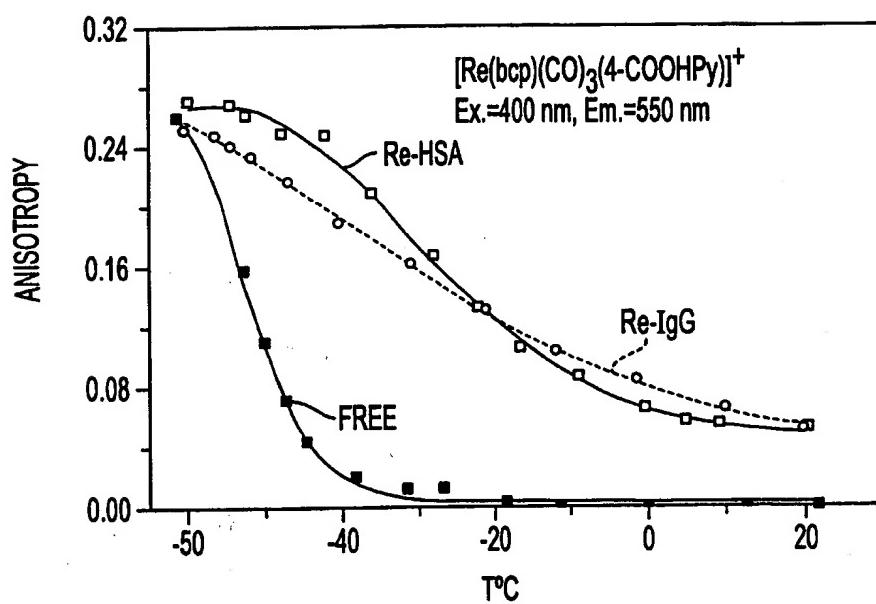
FIG. 28
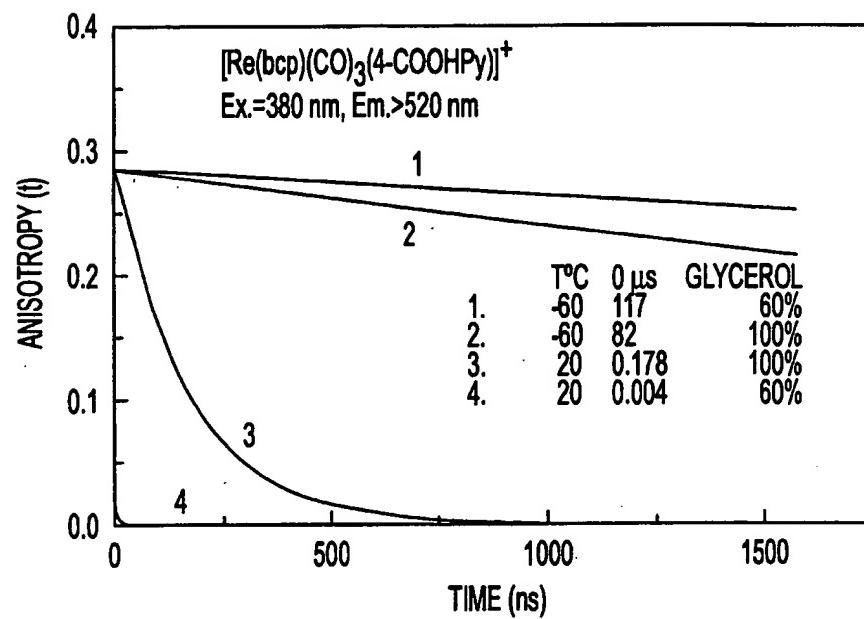
FIG. 29
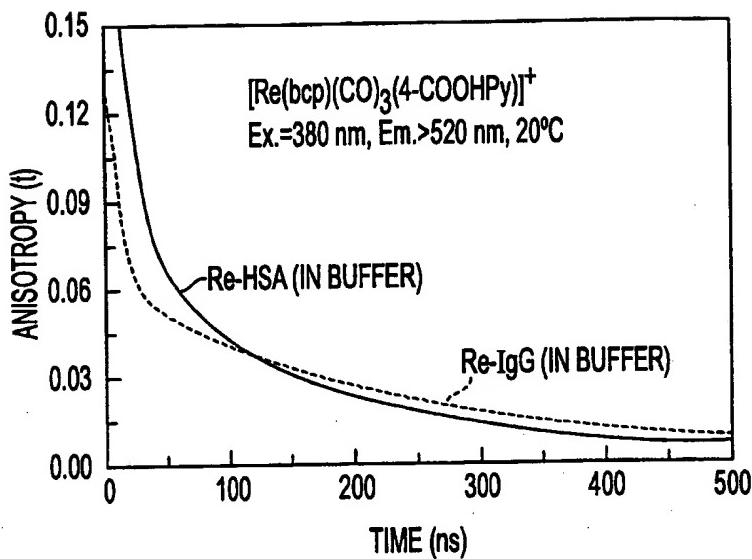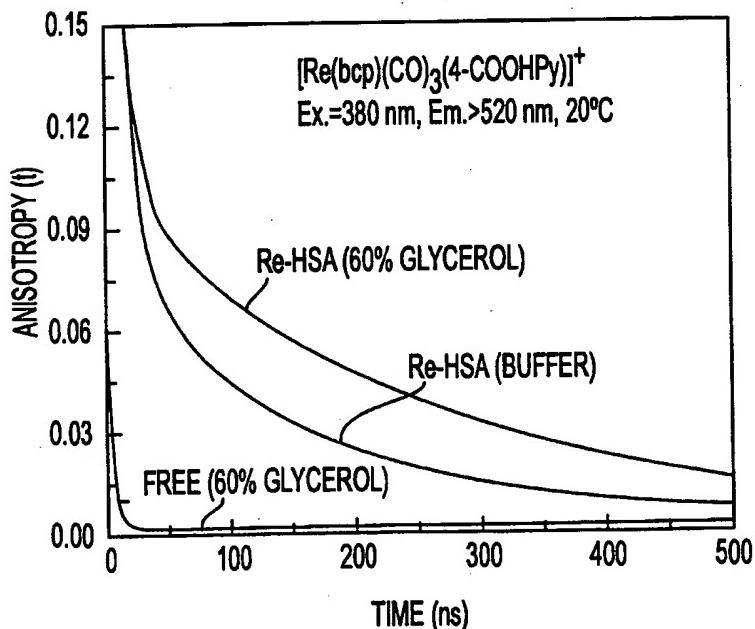
FIG. 30A

FIG. 30B

INTERNATIONAL SEARCH REPORT

A. CLASSIFICATION OF SUBJECT MATTER

IPC(6) :G01N 33/533
US CL :436/537, 536, 518, 546, 172; 422/82.07, 82.08, 82.09

According to International Patent Classification (IPC) or to both national classification and IPC

B. FIELDS SEARCHED

Minimum documentation searched (classification system followed by classification symbols)

U.S. : 436/537, 536, 518, 546, 172; 422/82.07, 82.08, 82.09

Documentation searched other than minimum documentation to the extent that such documents are included in the fields searched

Electronic data base consulted during the international search (name of data base and, where practicable, search terms used)

APS, WPIDS

C. DOCUMENTS CONSIDERED TO BE RELEVANT

Category*	Citation of document, with indication, where appropriate, of the relevant passages	Relevant to claim No.
Y	US 5,246,867 A (LAKOWICZ et al) 21 September 1993, see entire document.	1-20
Y	US 5,281,825 A (BERNDT et al) 25 January 1994, see entire document.	1-20
Y	US 5,624,847 A (LAKOWICZ et al) 29 April 1997, see entire document.	1-20
Y	US 5,628,310 A (RAO et al) 13 May 1997, see entire document.	1-20
Y	US 5,631,169 A (LAKOWICZ et al) 20 May 1997, see entire document.	1-20
Y	US 5,648,269 A (LAKOWICZ et al) 15 July 1997, see entire document.	1-20

[X] Further documents are listed in the continuation of Box C.   [ ] See patent family annex.

* Special categories of cited documents:	"T" later document published after the international filing date or priority date and not in conflict with the application but cited to understand the principle or theory underlying the invention
"A" document defining the general state of the art which is not considered to be of particular relevance	
"B" earlier document published on or after the international filing date	"X" document of particular relevance; the claimed invention cannot be considered novel or cannot be considered to involve an inventive step when the document is taken alone
"L" document which may throw doubts on priority claim(s) or which is cited to establish the publication date of another citation or other special reason (as specified)	"Y" document of particular relevance; the claimed invention cannot be considered to involve an inventive step when the document is combined with one or more other such documents, such combination being obvious to a person skilled in the art
"O" document referring to an oral disclosure, use, exhibition or other means	
"P" document published prior to the international filing date but later than the priority date claimed	"&" document member of the same patent family

Date of the actual completion of the international search	Date of mailing of the international search report
12 APRIL 1999	**14 MAY 1999**

Name and mailing address of the ISA/US	Authorized officer
Commissioner of Patents and Trademarks Box PCT Washington, D.C. 20231	BAO-THUY L. NGUYEN JOYCE BRIDGERS PARALEGAL SPECIALIST CHEMICAL MATRIX
Facsimile No. (703) 305-3230	Telephone No. (703) 308-0196

Form PCT/ISA/210 (second sheet)(July 1992)*

C (Continuation). DOCUMENTS CONSIDERED TO BE RELEVANT

Category*	Citation of document, with indication, where appropriate, of the relevant passages	Relevant to claim No.
Y	US 5,660,991 A (LAKOWICZ et al) 26 August 1997, see entire document.	1-20
Y,P	US 5,759,767 A (LAKOWICZ et al) 02 June 1998, see entire document.	1-20
Y,P	US 5,780,319 A (MAXFIELD WILSON et al) 14 July 1998, see entire document.	1-20

Form PCT/ISA/210 (continuation of second sheet)(July 1992)*